

Prompt neutrino fluxes from forward heavy quark production in $pp(pA)$

Anna Staśto



PennState
Eberly College of Science

Probing QCD at High Energy Frontier, ECT Trento, Italia, May 24, 2018*

Outline

- Motivation: ultrahigh energy neutrino astronomy
- Atmospheric neutrinos: conventional and prompt
- Cross section for charm production at forward rapidities: collinear, dipole and k_T factorization calculations
- Prompt neutrino fluxes

Work in collaboration with

A. Bhattacharya, R. Enberg, Y. S. Jeong, C. S. Kim, M. H. Reno, I. Sarcevic

Neutrino astronomy

- Universe not transparent to extragalactic photons with energy $> 10 \text{ TeV}$
- Weakly interacting: neutrinos can travel large distances without distortion

Interaction lengths (at 1 TeV):

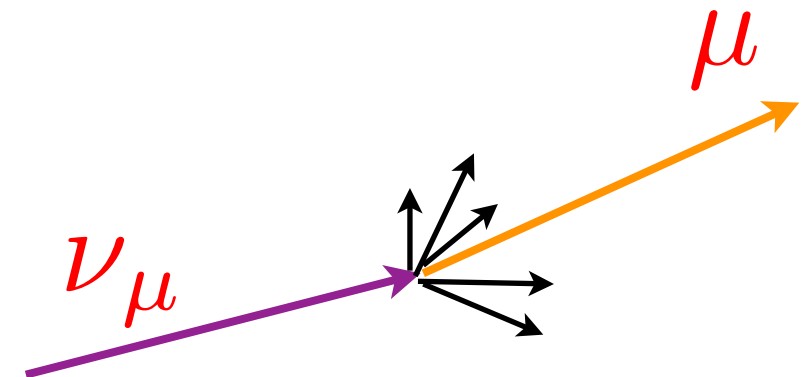
$$\mathcal{L}_{\text{int}}^{\gamma} \sim 100 \text{ g/cm}^2$$

$$\mathcal{L}_{\text{int}}^{\nu} \sim 250 \times 10^9 \text{ g/cm}^2$$

- Trajectories of protons and nuclei are distorted by the magnetic fields
- Neutrinos can point back to their sources

Angular
distortion

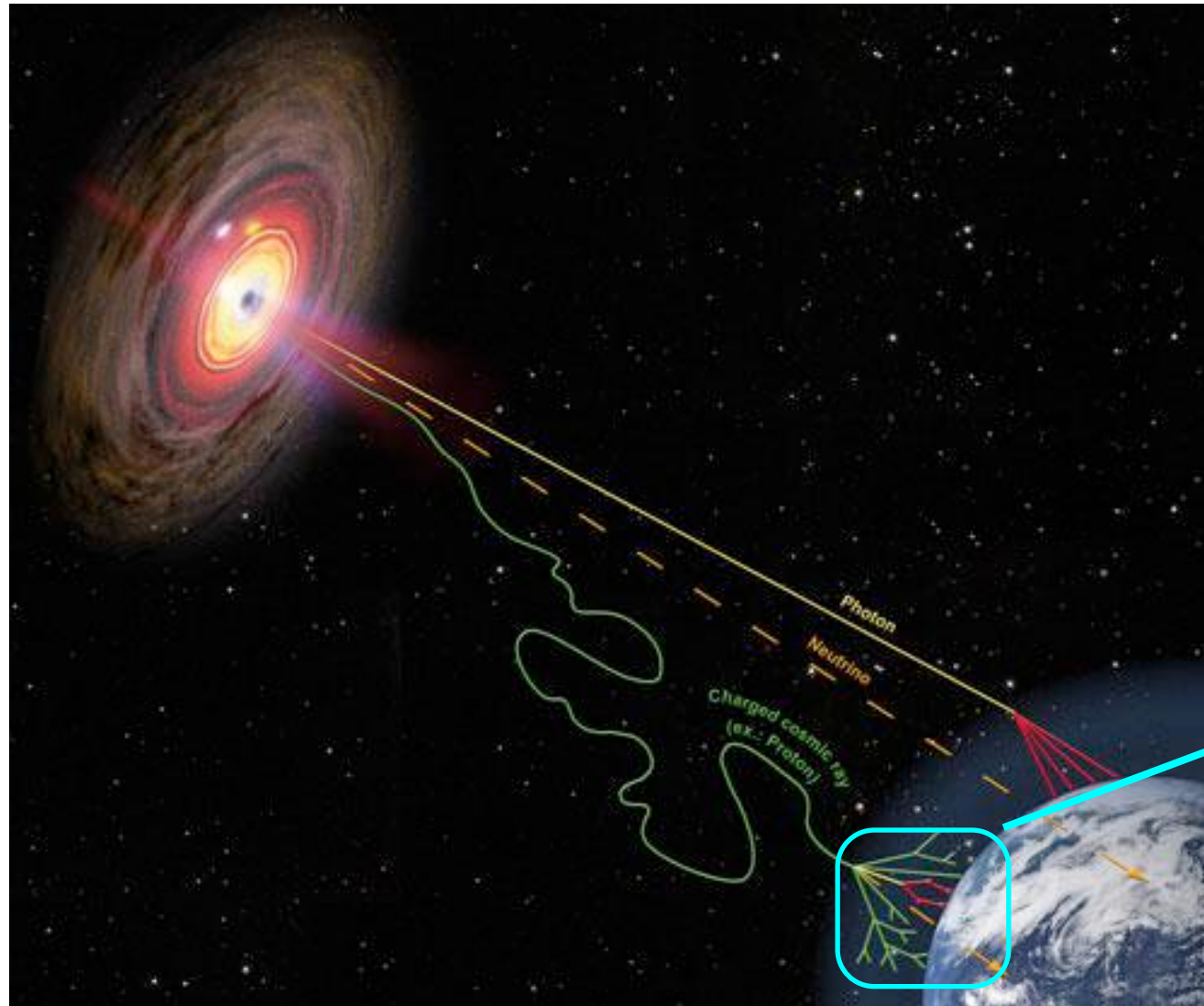
$$\delta\phi \simeq \frac{0.7^\circ}{(E_\nu/\text{TeV})^{0.7}}$$



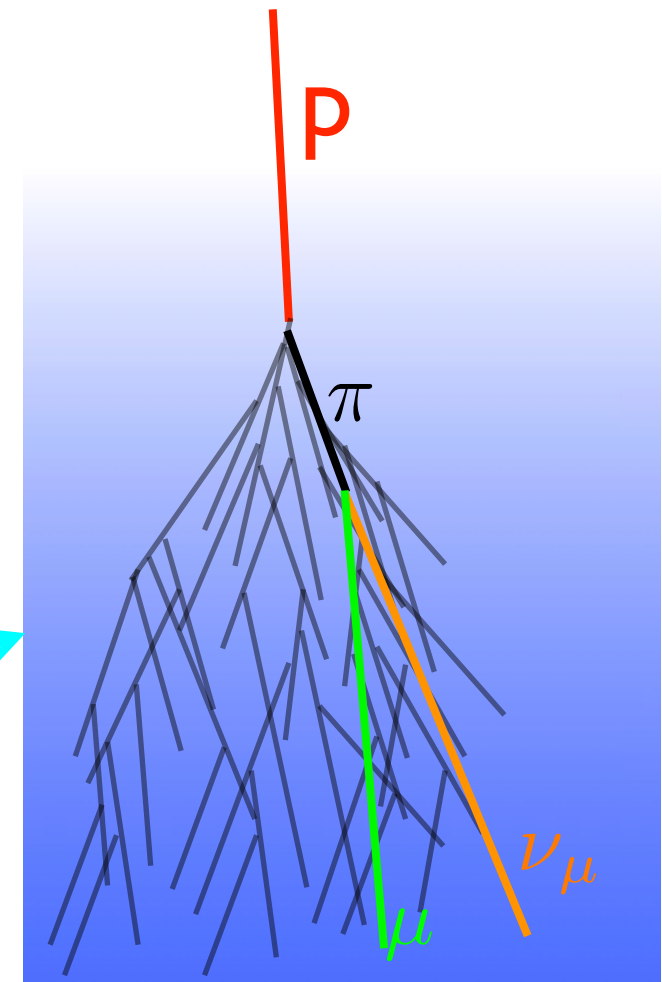
Sources of high energy neutrinos

- Atmospheric: interactions of cosmic rays with nuclei in the atmosphere.
- Interactions of cosmic rays with gas, for example around supernova remnants. Interaction with microwave background (GZK neutrinos).
- Production at some source: radio galaxies, Active Galactic Nuclei, Gamma Ray bursts.
- More exotic scenarios: WIMP annihilation (in the center of Sun or Earth), decays of metastable relic particles,...

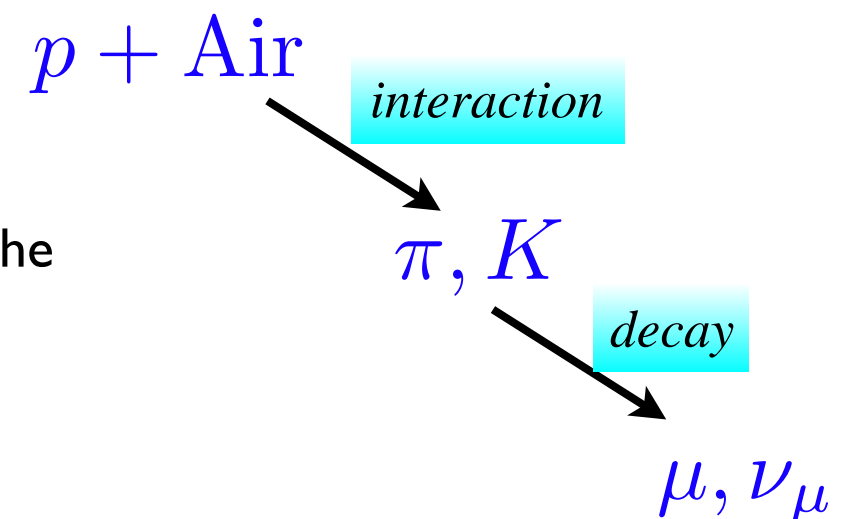
Atmospheric neutrinos



(credit: www.hap-astroparticle.org/ A. Chantelauze)



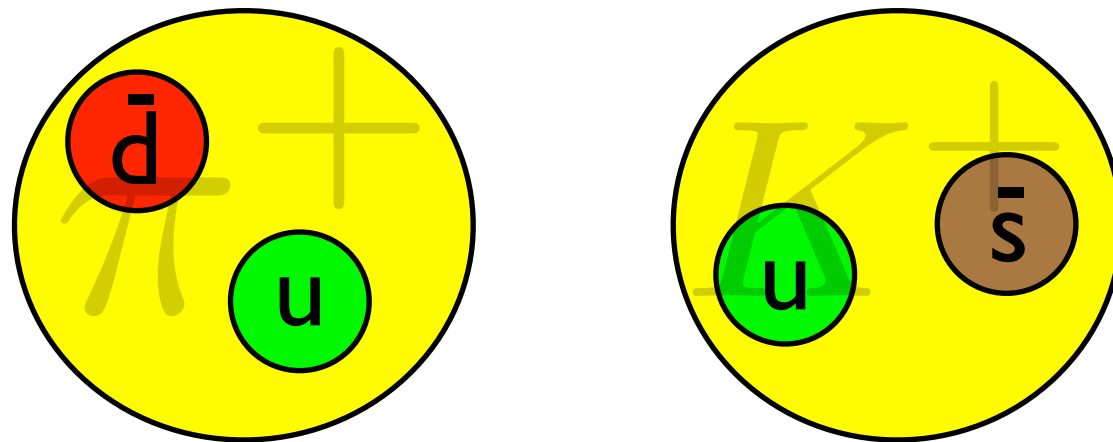
Neutrinos in the atmosphere originate from the interactions of cosmic rays (etc. protons) with nuclei.



Atmospheric neutrinos

- *Conventional*: decays of lighter mesons

$$\pi^{\pm}, K^{\pm}$$



Mean lifetime: $\tau \sim 10^{-8} \text{ s}$

Long lifetime: interaction occurs before decay

$$\mathcal{L}_{\text{int}} < \mathcal{L}_{\text{dec}}$$

Long-lived mesons
lose energy



Steeply falling flux of
neutrinos

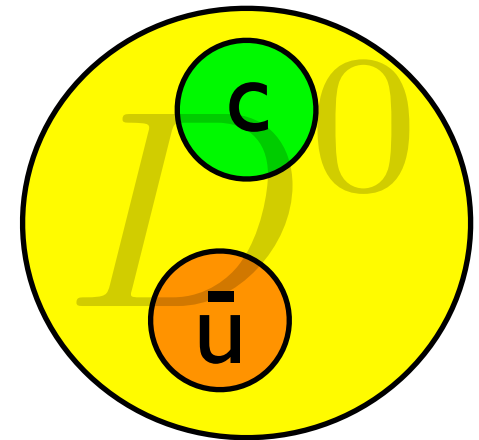
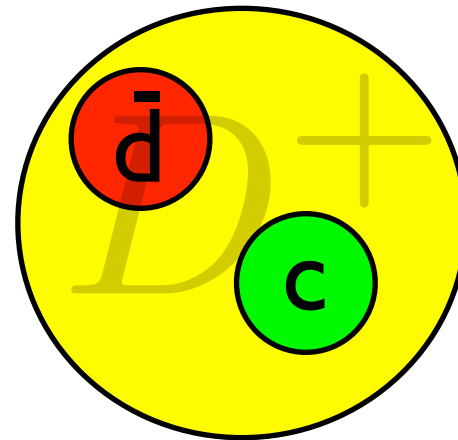
$$\Phi_{\nu} \sim E_{\nu}^{-3.7}$$

Prompt neutrinos

- *Prompt*: decays of heavier, charmed or bottom mesons

$$D^{\pm}, D^0, D_s$$

baryon Λ_c



Mean lifetime: $\tau \sim 10^{-12} \text{ s}$

Short lifetime: decay, no interaction

$$\mathcal{L}_{\text{int}} > \mathcal{L}_{\text{dec}}$$

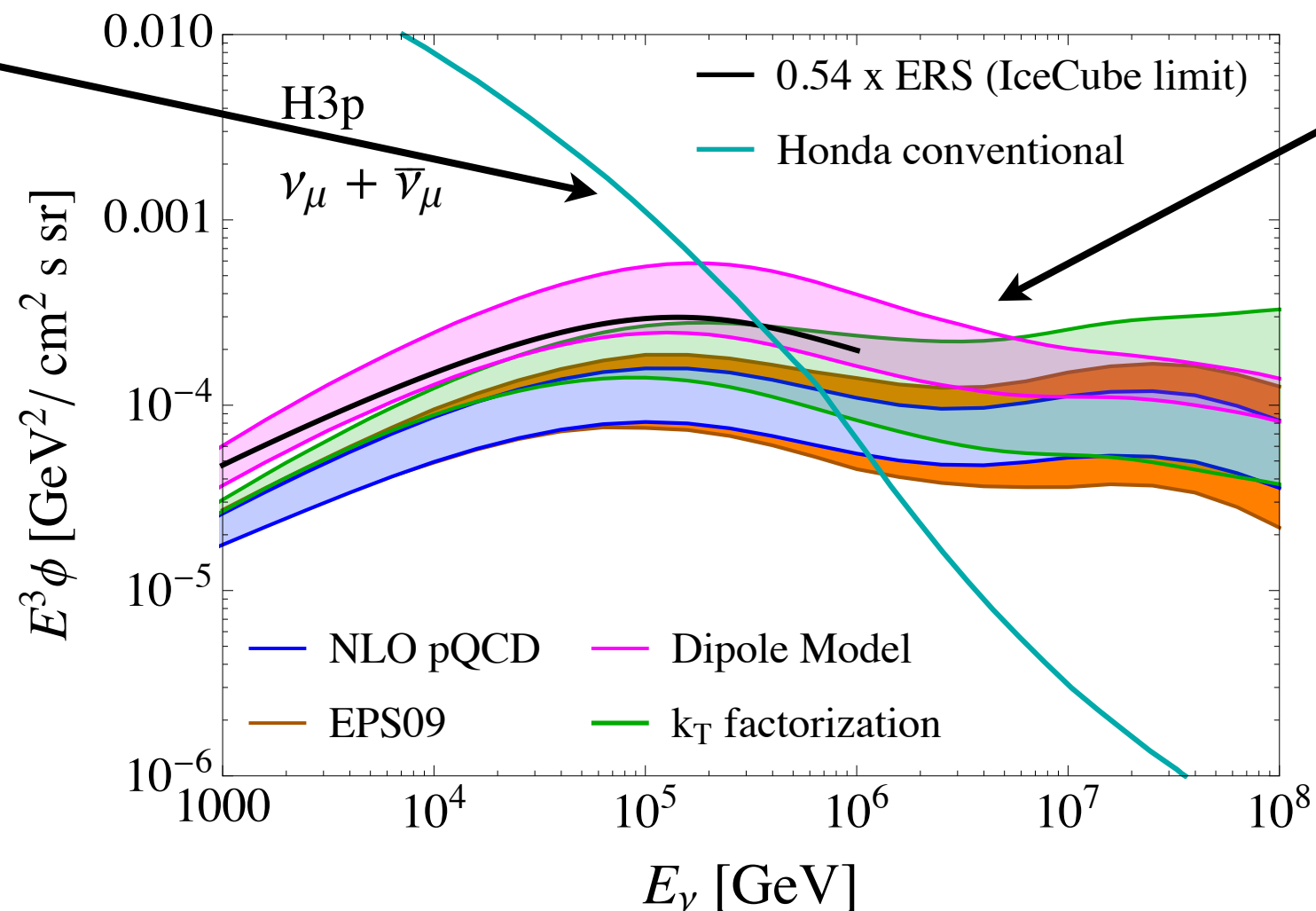
Flat flux, more energy
transferred to neutrino

$$\Phi_{\nu} \sim E_{\nu}^{-2.7}$$

Prompt vs conventional flux

High energy atmospheric neutrino flux as a function of energy

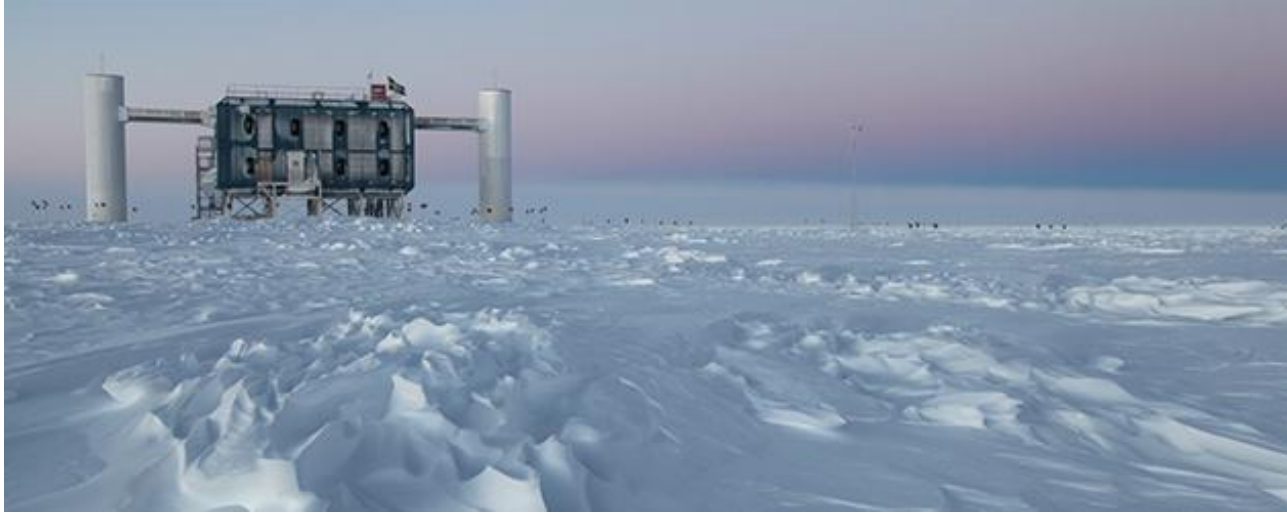
conventional:
decay of long
lived pions and
kaons: loose
energy.
Soft spectrum.



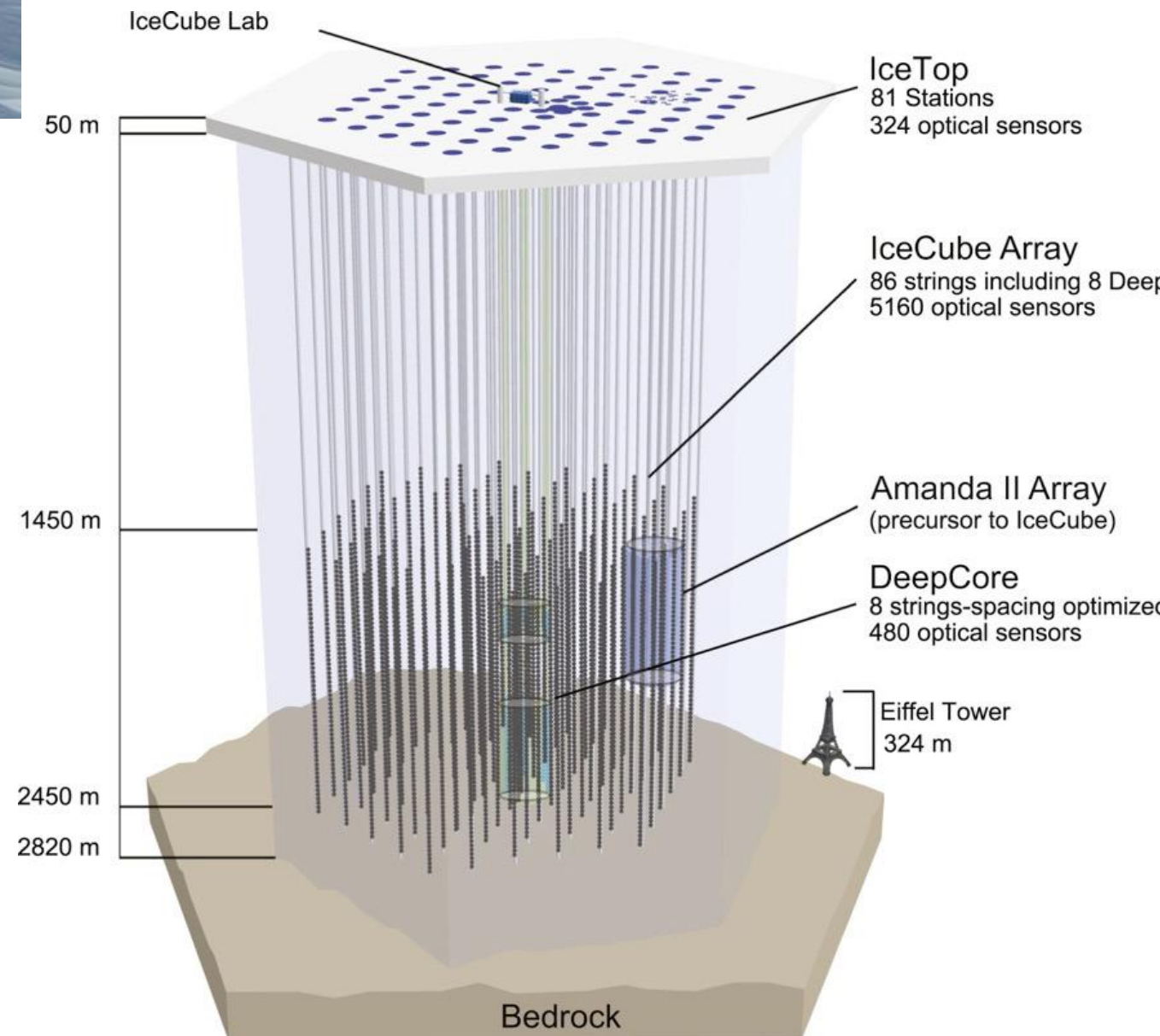
prompt: decay of
short lived charmed
mesons: do not loose
energy.
Hard spectrum.

- Conventional flux: constrained by the low energy neutrino data.
- Prompt flux: poorly known, large uncertainties. Essential to evaluate as it can dominate the background for searches for extraterrestrial high energy neutrinos.

IceCube



- UHE neutrinos measured in IceCube Antarctic detector
- Neutrinos detected using Cherenkov light produced by charged particles after neutrinos interact
- Sensitivity to high energy >100 GeV neutrinos (>10 GeV with Deep Core)



IceCube results

Two classes of events:

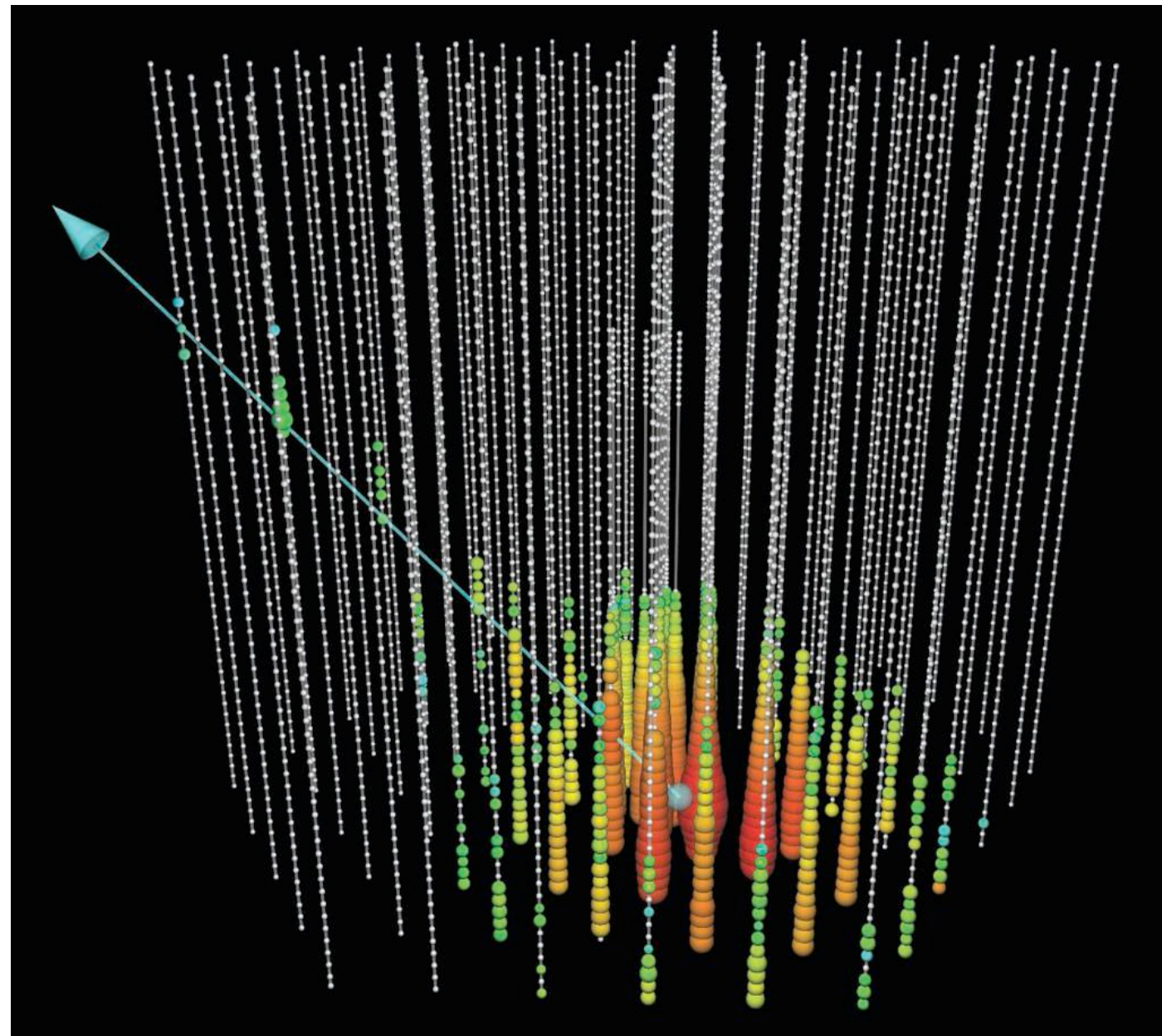
Showers: from secondary charged leptons and hadron dissociation

Tracks: events accompanied by an energetic muon (CC events with incoming ν_μ)

Evidence for High-Energy Extraterrestrial Neutrinos at the IceCube Detector

IceCube Collaboration*

SCIENCE VOL 342 22 NOVEMBER 2013

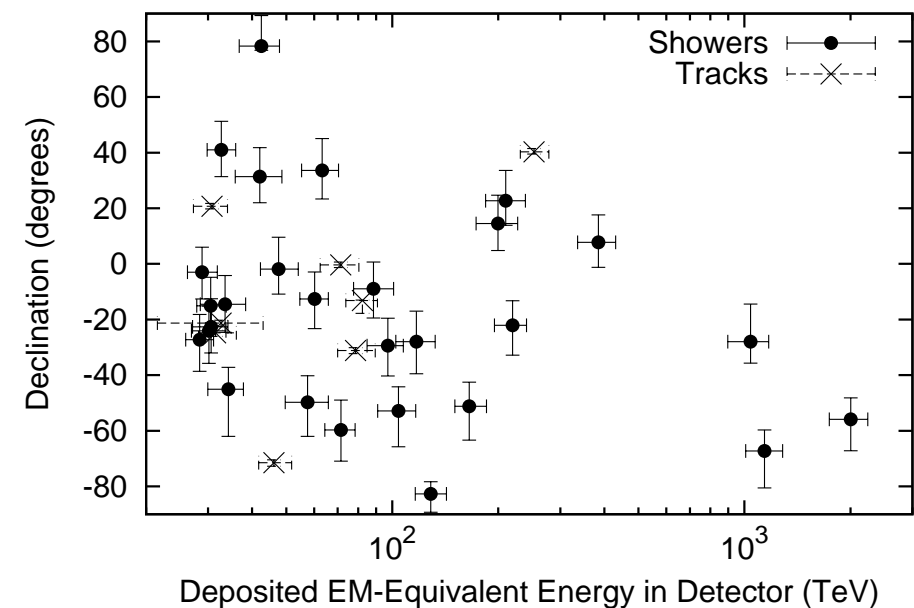
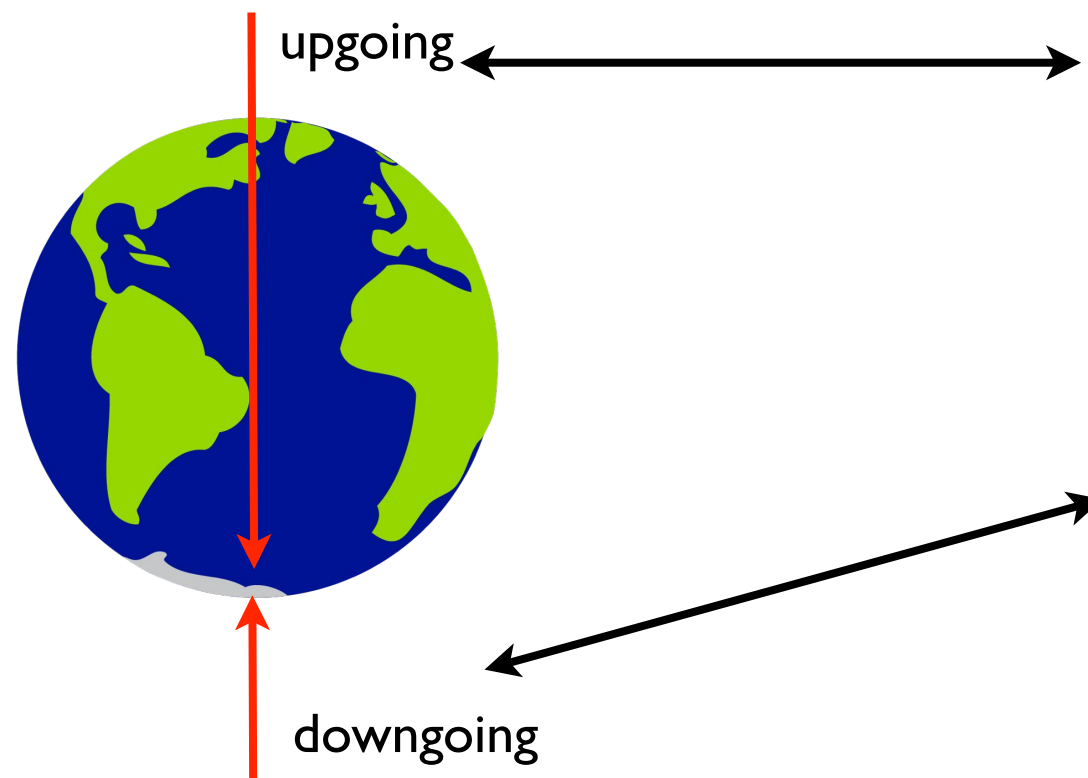


A 250 TeV neutrino interaction in IceCube. At the neutrino interaction point (bottom), a large particle shower is visible, with a muon produced in the interaction leaving up and to the left. The direction of the muon indicates the direction of the original neutrino.

IceCube results

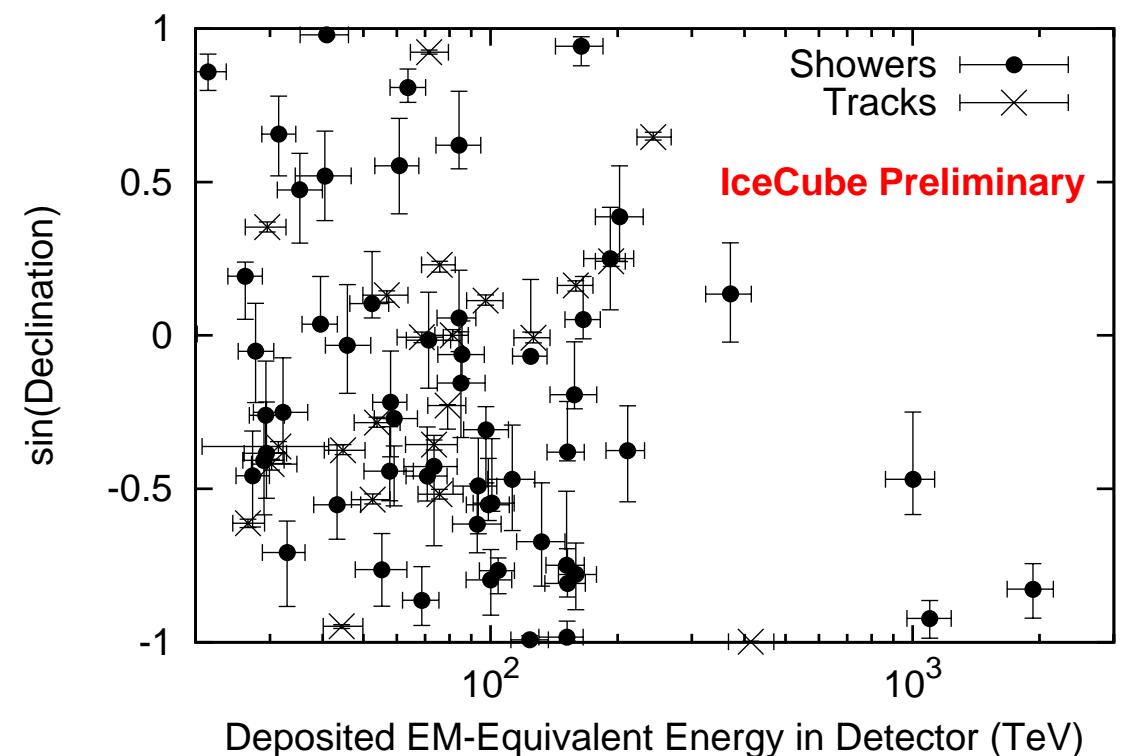
IceCube Coll. Phys.Rev.Lett. 113 (2014) 101101; Observation of High-Energy Astrophysical Neutrinos in Three Years of IceCube Data

988 day sample, 37 events observed (after selection with entering muon veto) with energies between 30-2000 TeV



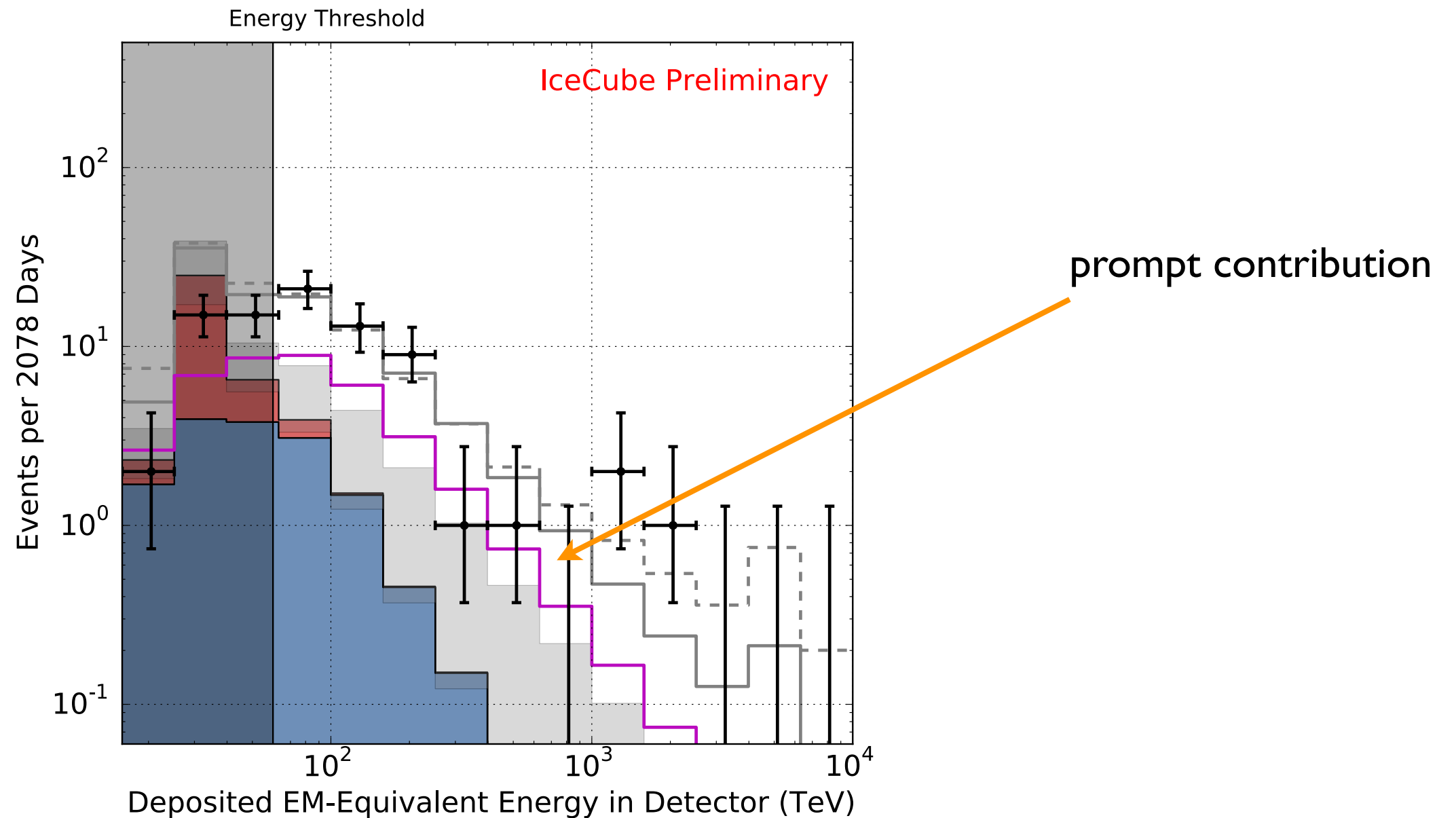
6 year data, 2078 days, 82 events above 30TeV

C. Kopper, ICRC2017, arXiv:1710.01191

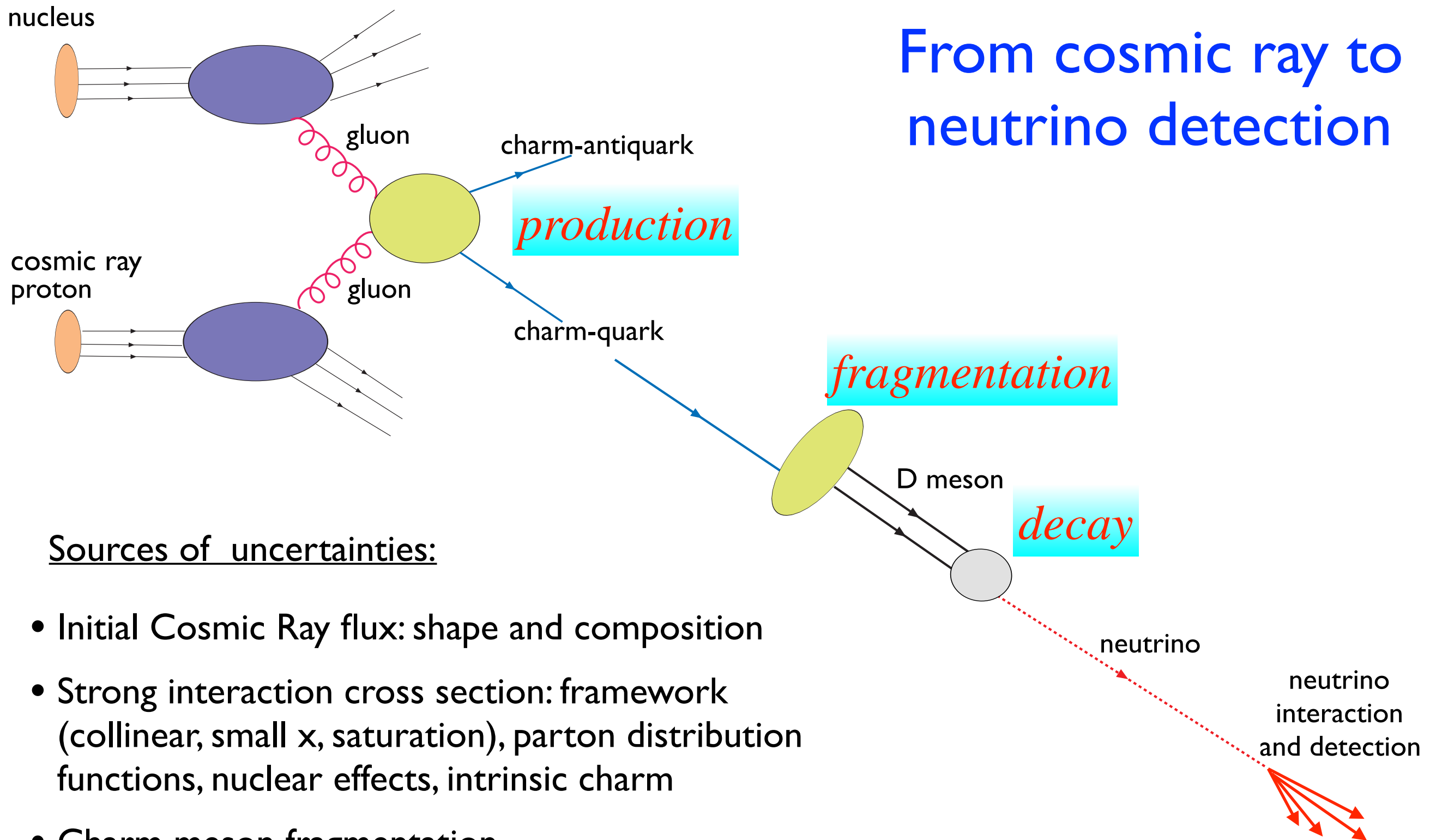


Motivation

- Atmospheric origin of signal excess is excluded with 5 sigma.
- Still, prompt neutrino is the most background for the astrophysical flux of neutrinos. It dominates the uncertainty at high energies.
- Neutrino production at these range of energies is sensitive to small x physics.



From cosmic ray to neutrino detection



Sources of uncertainties:

- Initial Cosmic Ray flux: shape and composition
- Strong interaction cross section: framework (collinear, small x , saturation), parton distribution functions, nuclear effects, intrinsic charm
- Charm meson fragmentation
- Decay
- Interaction cross section of neutrino

Frameworks for heavy quark production

- Standard NLO perturbative QCD collinear calculation.
- High-energy factorization with small x BFKL/DGLAP resummed evolution, including saturation effects (through nonlinear evolution equation).
- Small x dipole model with saturation.

Also:

Nuclear corrections.

b quark contribution.

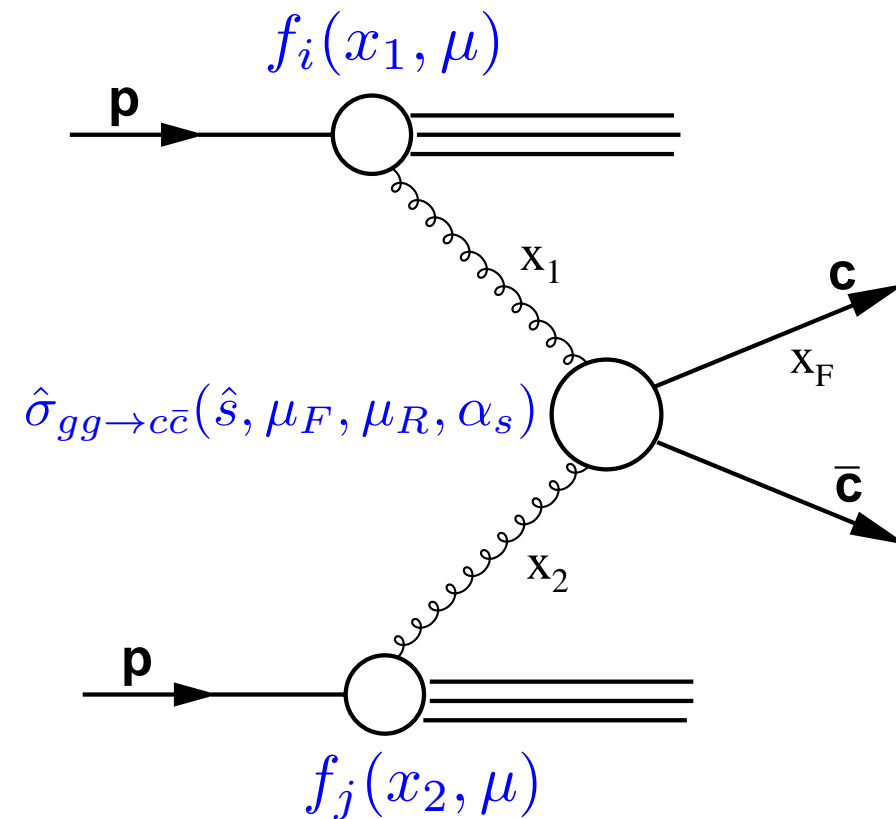
Heavy quark production in hadron collisions

Schematic representation of charm production in pp scattering:

$f_i(x, \mu)$ parton distribution function at scale μ
 parametrized at scale μ_0
 evolved to higher scales with QCD evolution equations

x_1, x_2 longitudinal momentum fractions (of a proton momentum) of gluons participating in a scattering process

$\hat{\sigma}_{gg \rightarrow c\bar{c}}(\hat{s}, \mu_F, \mu_R, \alpha_s)$ partonic cross section calculable in a perturbative way in QCD



Factorization formula for cross section:

$$\frac{d\sigma^{pp \rightarrow c+X}}{dx_F} = \sum_{i,j} f_i(x_1, \mu_F) \otimes \hat{\sigma}_{gg \rightarrow c\bar{c}}(\hat{s}, m_c, \mu_F, \mu_R) \otimes f_j(x_2, \mu_F)$$

pQCD collinear calculation

$$\frac{d\sigma^{pp \rightarrow c+X}}{dx_F} = \sum_{i,j} f_i(x_1, \mu_F) \otimes \hat{\sigma}_{gg \rightarrow c\bar{c}}(\hat{s}, m_c, \mu_F, \mu_R) \otimes f_j(x_2, \mu_F)$$

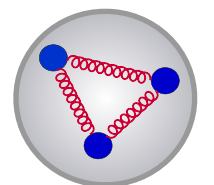
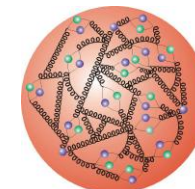
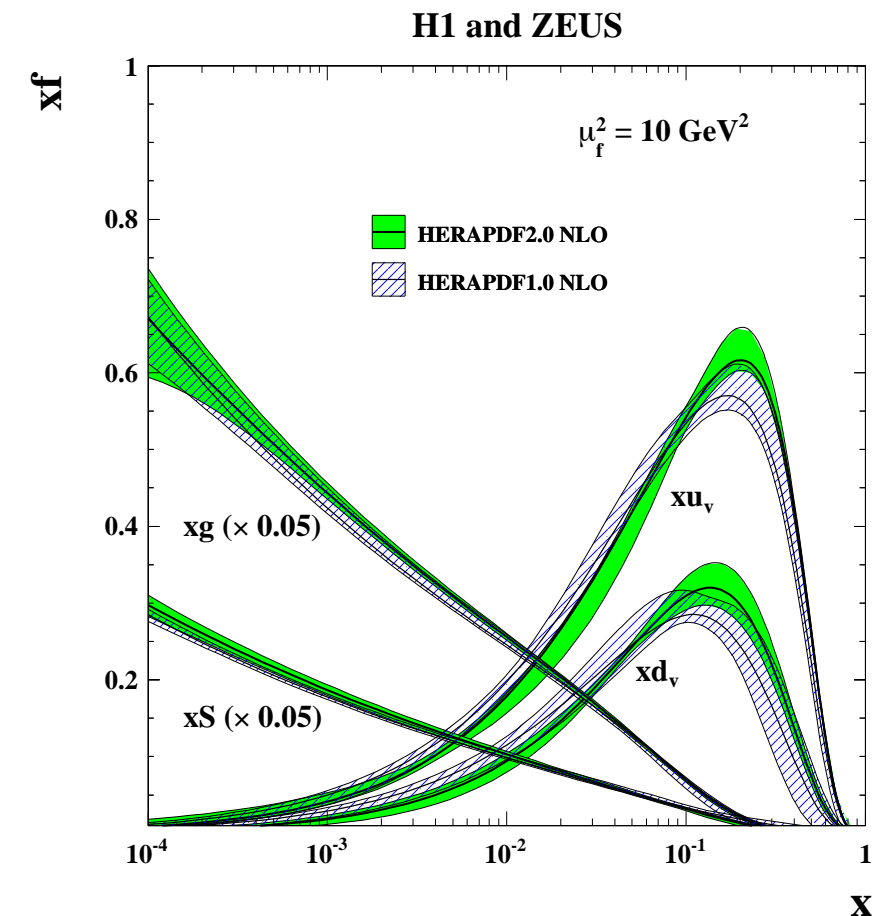
For the cosmic ray interactions we are interested in the forward production: charm quark is produced with very high fraction of the momentum of the incoming cosmic ray projectile.

Other participating gluon will have very small fraction of longitudinal momentum:

$$x_F \simeq \frac{E_c}{E_p} \quad x_F \gg x_2 \quad x_2 \sim \frac{M_{c\bar{c}}^2}{x_F s}$$

$$s \gg M_{c\bar{c}}^2$$

The cross section is sensitive to the domain of parton densities which are at very small values of x . This is poorly constrained region.



Hybrid k_T factorization calculation

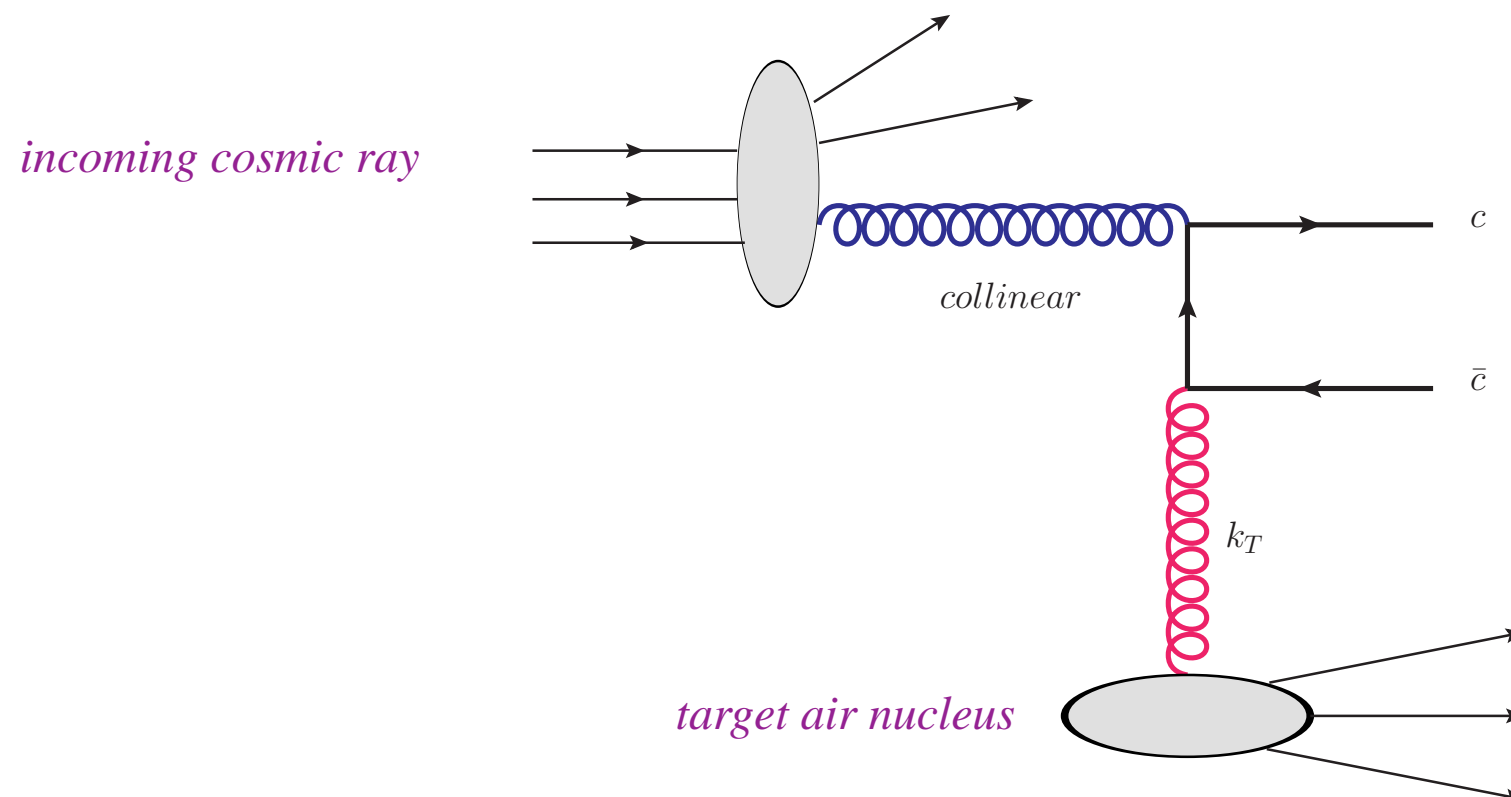
Use k_T factorization for heavy quarks with off-shell gluon and unintegrated parton density.
Suitable for the high energy - low x regime.

Catani, Ciafaloni, Hautmann; Collins, Ellis; Levin, Ryskin, Shabelski, Shuvaev

Since it is forward production, use 'hybrid' calculation: treat large x gluon as collinear, and small x gluon as off-shell.

$$\sigma(pp \rightarrow q\bar{q}X) = \int \frac{dx_1}{x_1} \frac{dx_2}{x_2} dz dx_F \delta(zx_1 - x_F) \boxed{x_1 g(x_1, M_F)} \quad \text{collinear gluon}$$

$$\times \int \frac{dk_T^2}{k_T^2} \hat{\sigma}^{\text{off}}(z, \hat{s}, k_T) \boxed{f(x_2, k_T^2)} \quad \text{off-shell gluon with } k_T \text{ dependence}$$



Hybrid k_T factorization calculation

Unintegrated gluon density obtained from the resummed small x evolution equation with non-linear term:

$$\begin{aligned}
 f(x, k^2) = & \tilde{f}^{(0)}(x, k^2) + \text{BFKL term with kinematical constraint} \\
 & + \frac{\alpha_s(k^2) N_c}{\pi} k^2 \int_x^1 \frac{dz}{z} \int_{k_0^2} \frac{dk'^2}{k'^2} \left\{ \frac{f(\frac{x}{z}, k'^2) \Theta(\frac{k^2}{z} - k'^2) - f(\frac{x}{z}, k^2)}{|k'^2 - k^2|} + \frac{f(\frac{x}{z}, k^2)}{|4k'^4 + k^4|^{\frac{1}{2}}} \right\} + \\
 & \text{DGLAP with non-singular splitting} \left(+ \frac{\alpha_s(k^2) N_c}{\pi} \int_x^1 dz \bar{P}_{gg}(z) \int_{k_0^2}^{k^2} \frac{dk'^2}{k'^2} f(\frac{x}{z}, k'^2) - \right. \\
 & \left. - \left(1 - k^2 \frac{d}{dk^2} \right)^2 \frac{k^2}{R^2} \int_x^1 \frac{dz}{z} \left[\int_{k^2}^{\infty} \frac{dk'^2}{k'^4} \alpha_s(k'^2) \ln \left(\frac{k'^2}{k^2} \right) f(z, k'^2) \right]^2 \right) \\
 & \text{non-linear term}
 \end{aligned}$$

Nonlinear term responsible for taming the growth of the gluon density

Unintegrated parton density fitted to the inclusive structure function data at HERA

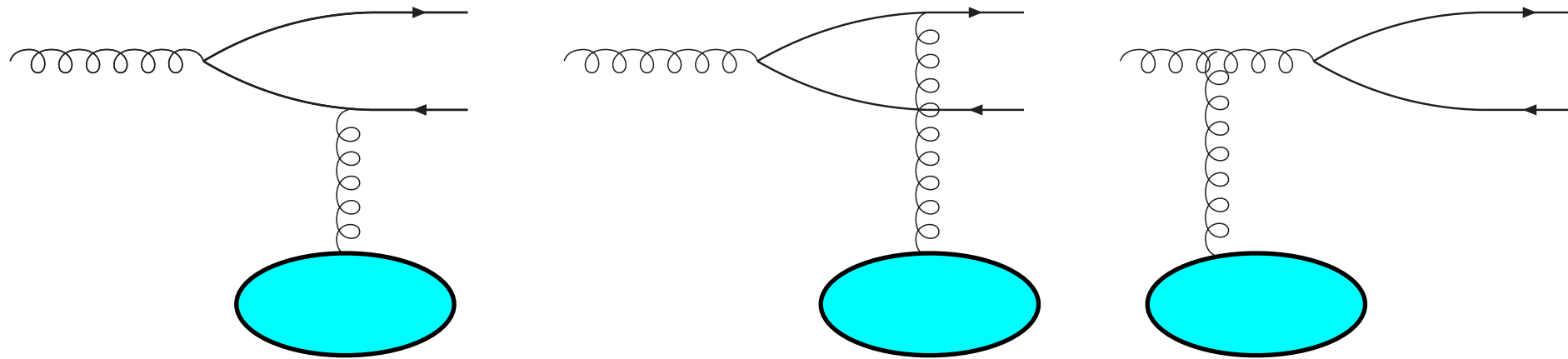
Two scenarios: linear and non-linear. Included A dependence in the nonlinear term.

Kutak, Sapeta; based on KMS (Kwiecinski, Martin, AS)

Dipole model calculation

Mueller; Nikolaev, Zakharov; Kopeliovich, Tarasov; Raufeisen, Peng

At high energy the production of the heavy quark pair is viewed as interaction of color dipole:



Gluon fluctuation into heavy quark-antiquark pair : color dipole
Interaction of the color dipole with the hadronic target.

Advantage of this framework: saturation and nuclear effects can be easily included as multiple scattering of the color dipole off the target.

Dipole model calculation

Heavy quark cross section in the dipole model:

$$\sigma(pp \rightarrow q\bar{q}X) \simeq \int dy x_1 g(x_1, M_F) \sigma^{gp \rightarrow q\bar{q}X}(x_2, M_R, Q^2 = 0)$$

Partonic cross section:

$$\sigma^{gp \rightarrow q\bar{q}X}(x, M_R, Q^2) = \int dz d^2\vec{r} |\Psi_g^q(z, \vec{r}, M_R, Q^2)|^2 \sigma_d(x, \vec{r})$$

Dipole cross section:

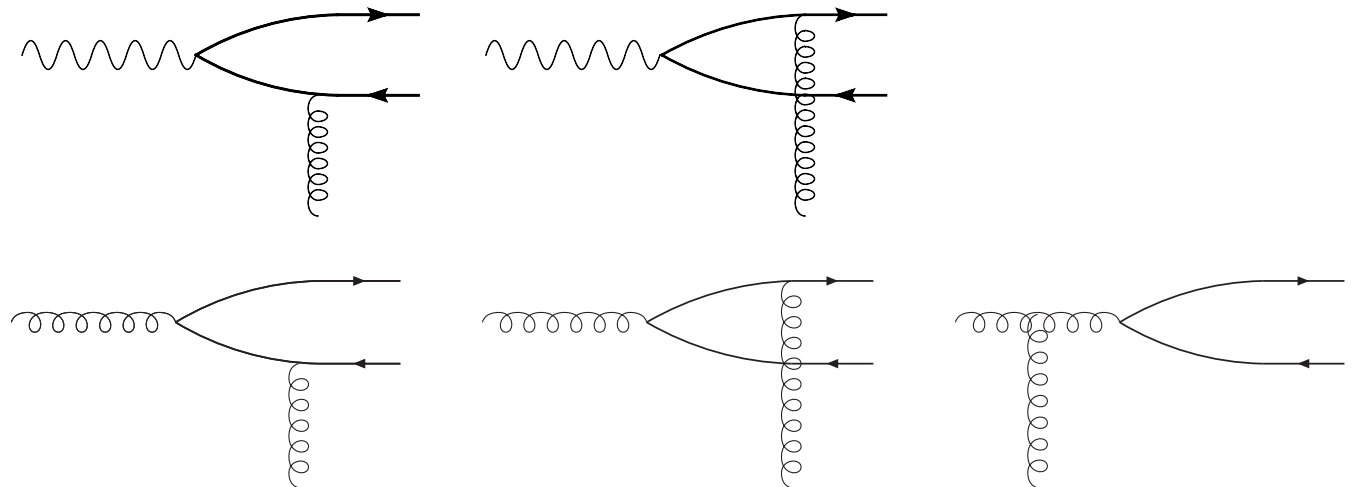
$$\sigma_d(x, \vec{r}) = \frac{9}{8} [\sigma_{d,em}(x, z\vec{r}) + \sigma_{d,em}(x, (1-z)\vec{r})] - \frac{1}{8} \sigma_{d,em}(x, \vec{r})$$

$$\sigma_{d,em}(x, \vec{r})$$

color singlet dipole

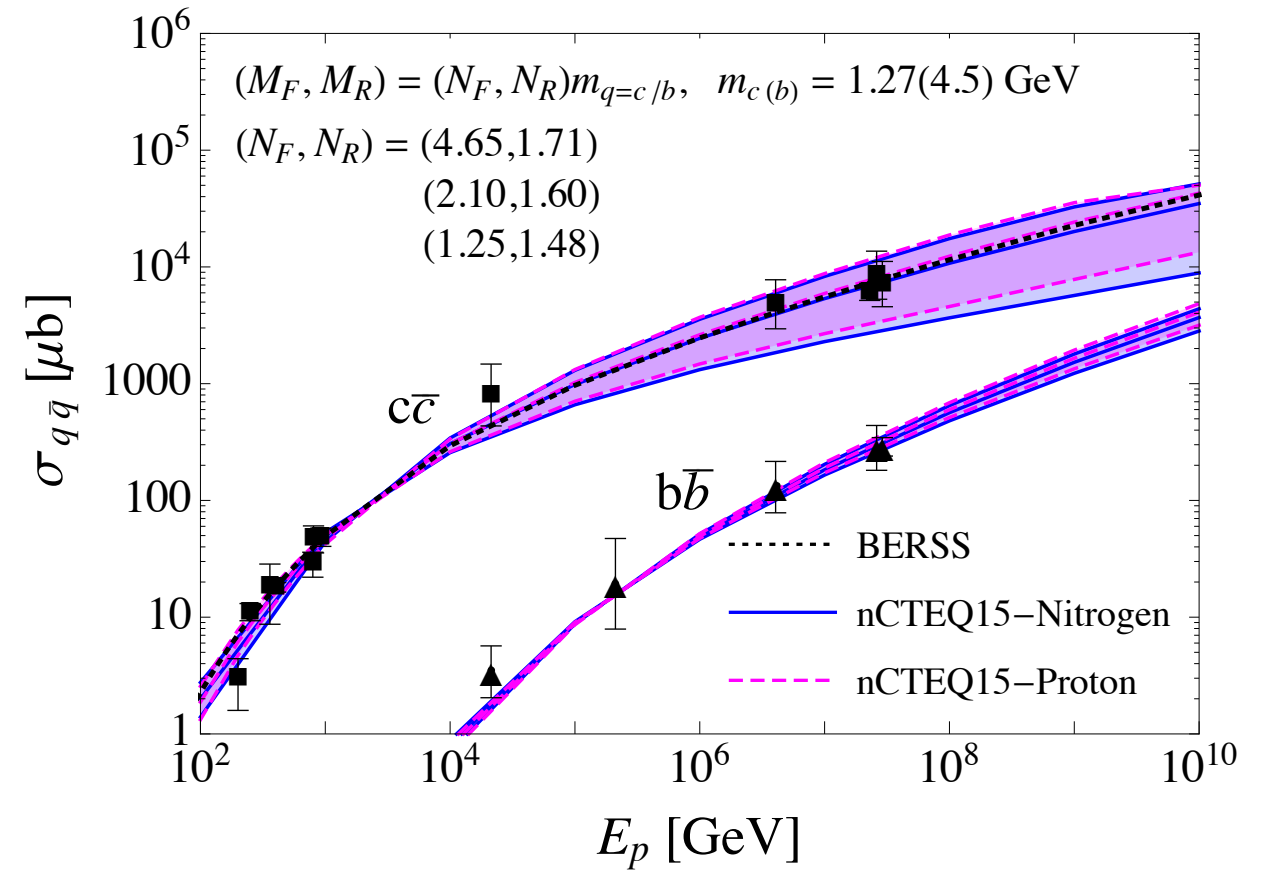
$$\sigma_d(x, \vec{r})$$

gluon dipole



Total charm production cross section

- NLO collinear calculation, HVQ, *Nason, Dawson, Ellis; Mangano, Nason, Ridolfi*
- Default parton distribution set is CT15 Central.
- Charm quark mass $m_c = 1.27$ GeV
- Variation of factorization and renormalization scales with respect to charm quark mass. Using range provided by *Nelson, Vogt, Frawley*
- Magenta-free nucleons, blue-nitrogen
- Comparison with RHIC and LHC data. Data are extrapolated with NLO QCD from measurements in the limited phase space region.



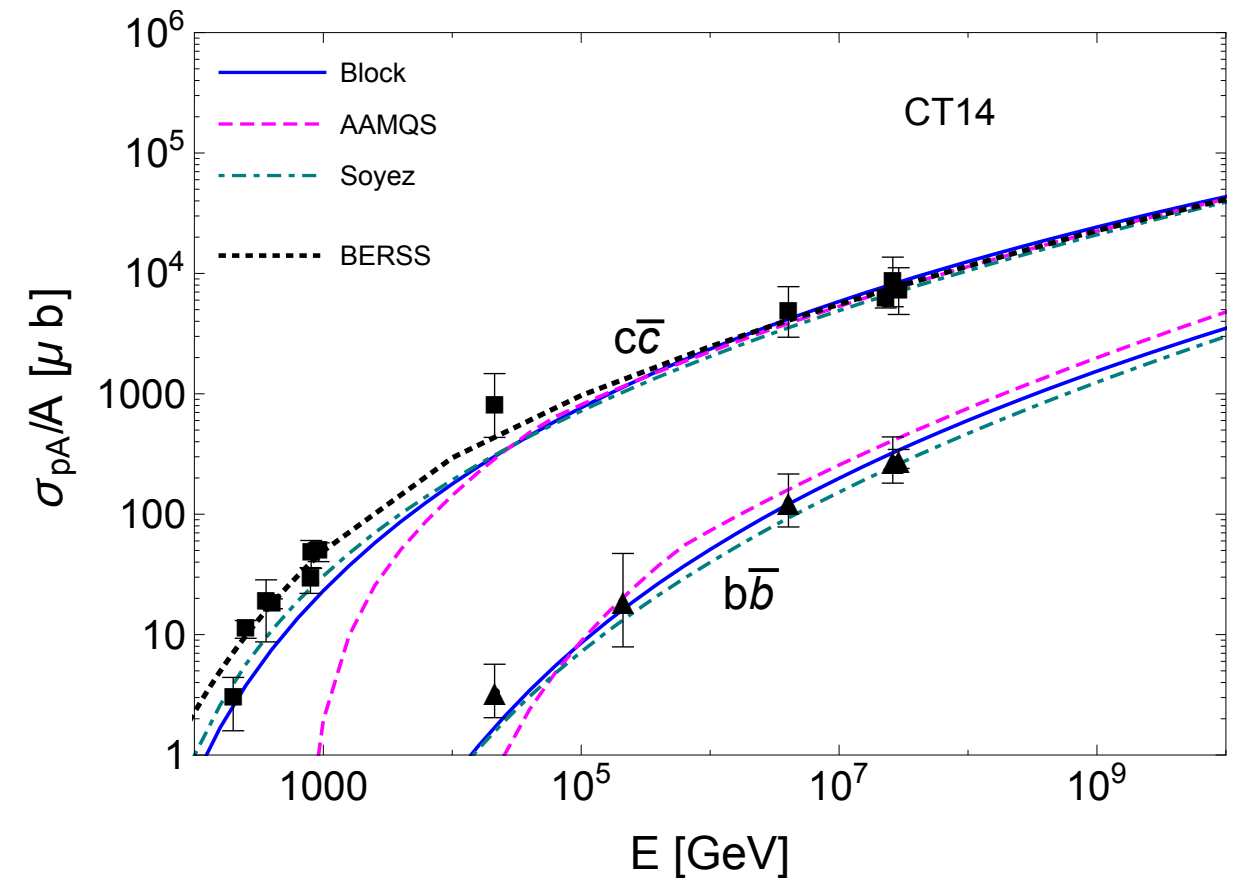
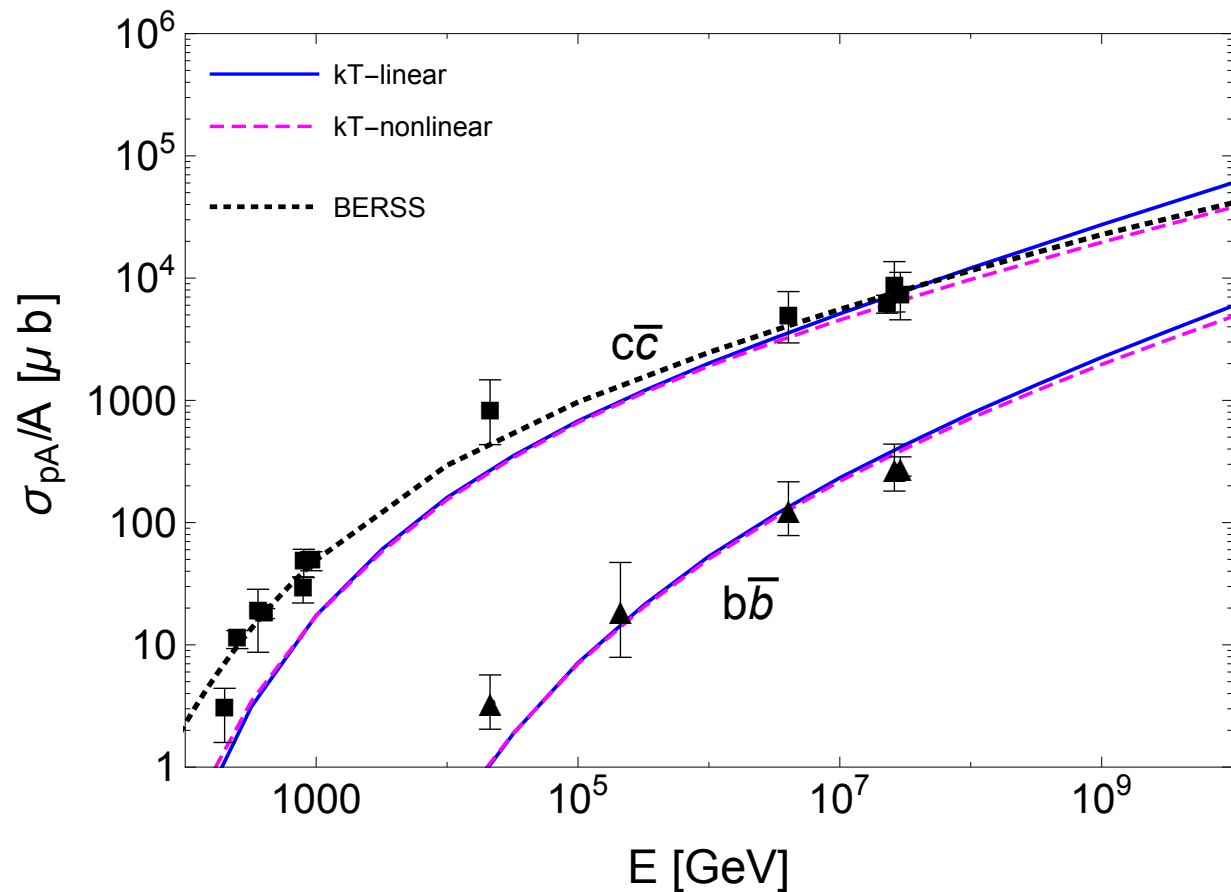
| Expt. | \sqrt{s} [TeV] | σ [mb] |
|-------------|------------------|---|
| PHENIX [31] | 0.20 | $0.551^{+0.203}_{-0.231}$ (sys) |
| STAR [32] | 0.20 | 0.797 ± 0.210 (stat) $^{+0.208}_{-0.295}$ (sys) |
| ALICE [27] | 2.76 | 4.8 ± 0.8 (stat) $^{+1.0}_{-1.3}$ (sys) ± 0.06 (BR) ± 0.1 (frag) ± 0.1 (lum) $^{+2.6}_{-0.4}$ (extrap) |
| ALICE [27] | 7.00 | 8.5 ± 0.5 (stat) $^{+1.0}_{-2.4}$ (sys) ± 0.1 (BR) ± 0.2 (frag) ± 0.3 (lum) $^{+5.0}_{-0.4}$ (extrap) |
| ATLAS [28] | 7.00 | 7.13 ± 0.28 (stat) $^{+0.90}_{-0.66}$ (sys) ± 0.78 (lum) $^{+3.82}_{-1.90}$ (extrap) |
| LHCb [30] | 7.00 | 6.100 ± 0.930 |

Table 1: Total cross-section for $pp(pN) \rightarrow c\bar{c}X$ in hadronic collisions, extrapolated based on NLO QCD by the experimental collaborations from charmed hadron production measurements in a limited phase space region.

Total charm production cross section

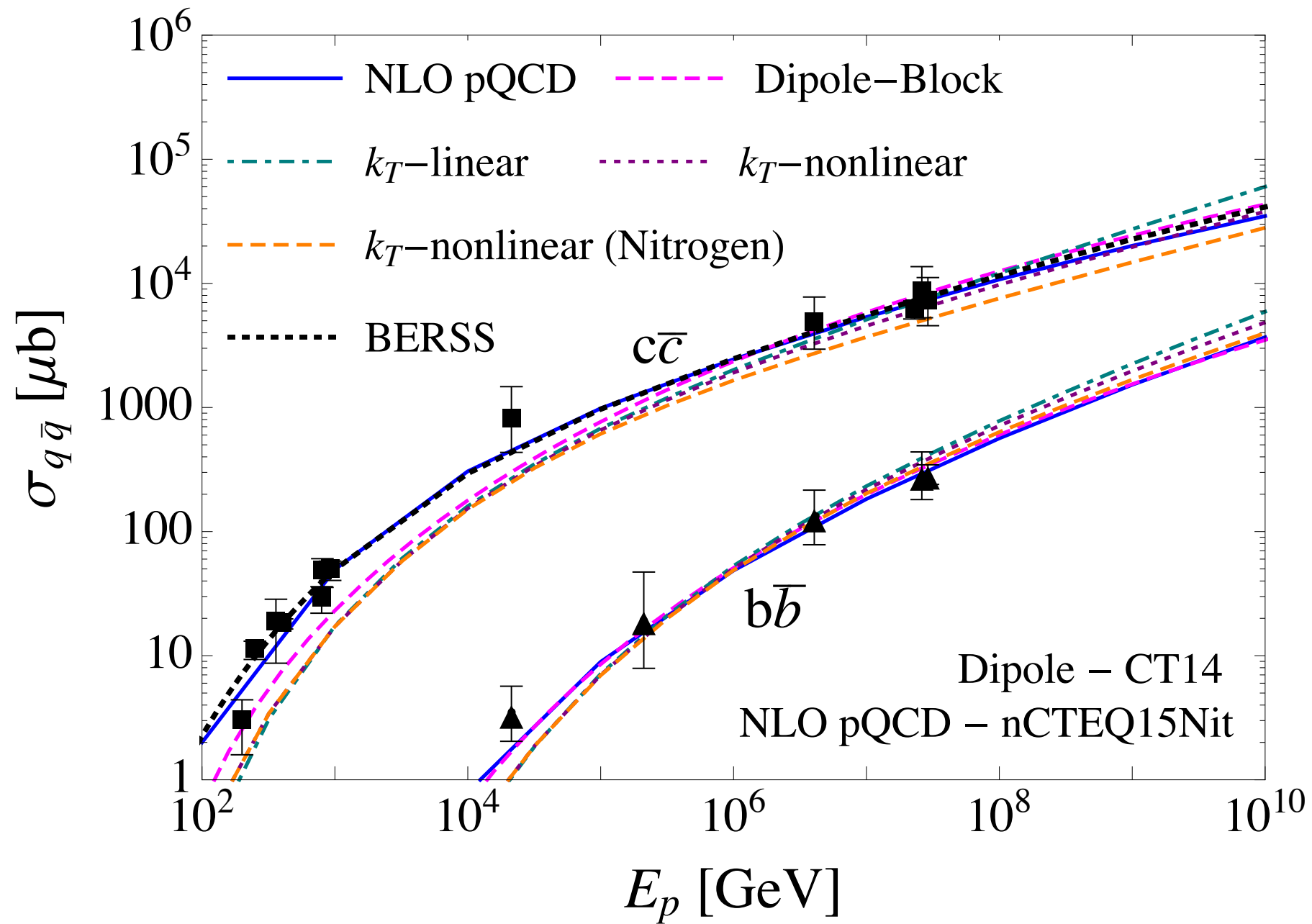
k_T

dipole model



- BERSS: *Bhattacharya, Enberg, Reno, Stasto, Sarcevic*: previous NLO calculation
- AAMQS, *Albacete, Armesto, Milhano, Quiroga-Arias, Salgado*: rcBK
- *Soyez*: based on *Iancu, Itakura, Munier* parametrization inspired by BK solution
- *Block*: phenomenological parametrization of the structure function
- k_T calculation underestimates data at low energy.
- Need additional diagrams there (or energy dependent K-factor).

Total charm production cross section

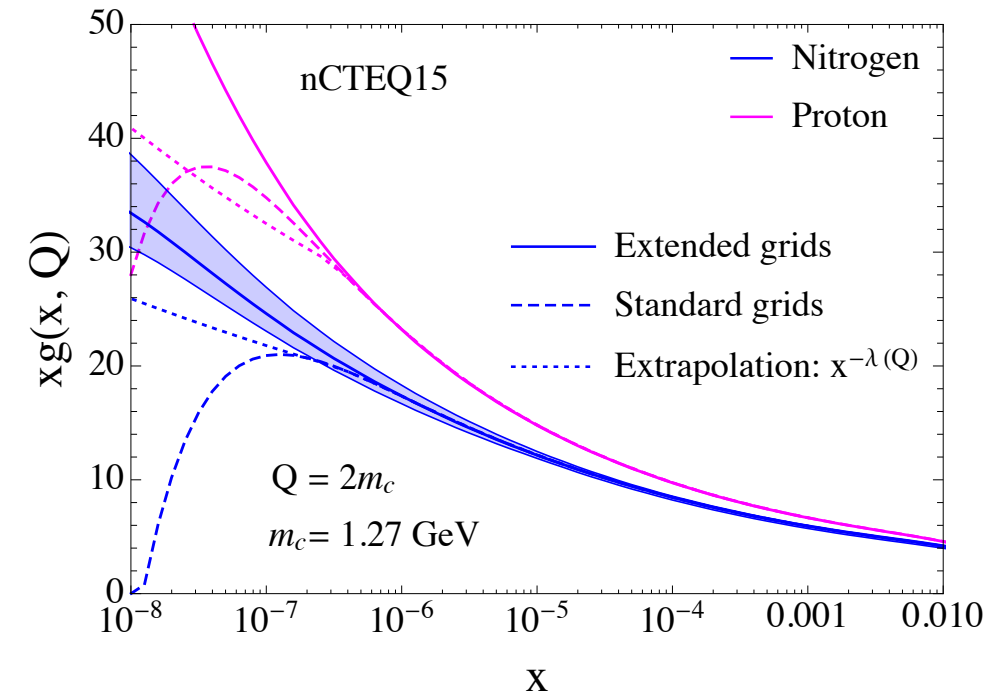
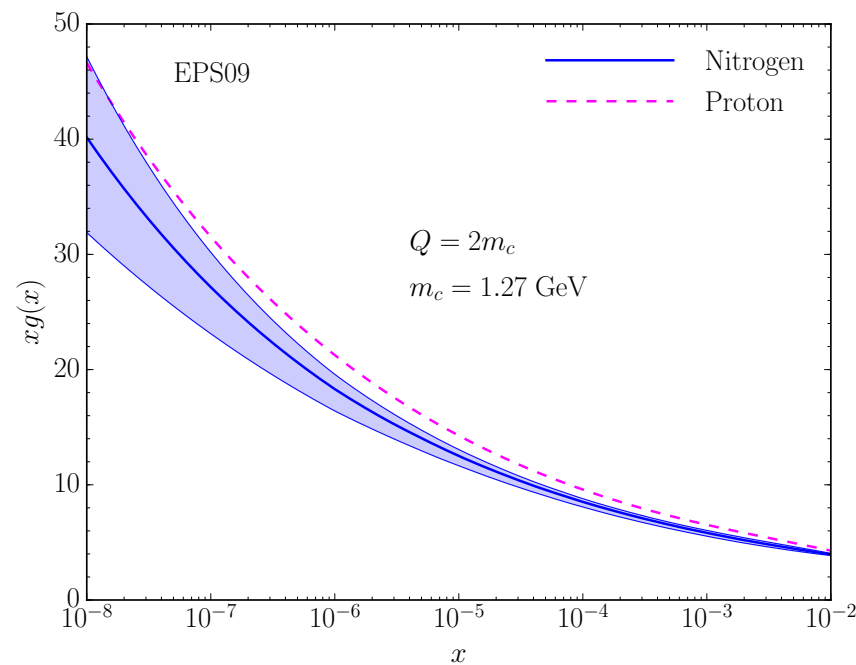


- Total charm production cross section described well by all models (at high energy).
- Nuclear effects very small for the total cross section.

Nuclear corrections

NLO pQCD

Use of nuclear PDFs,
nCTEQ and EPS



Dipole model

Glauber-Gribov formalism for nuclear rescattering

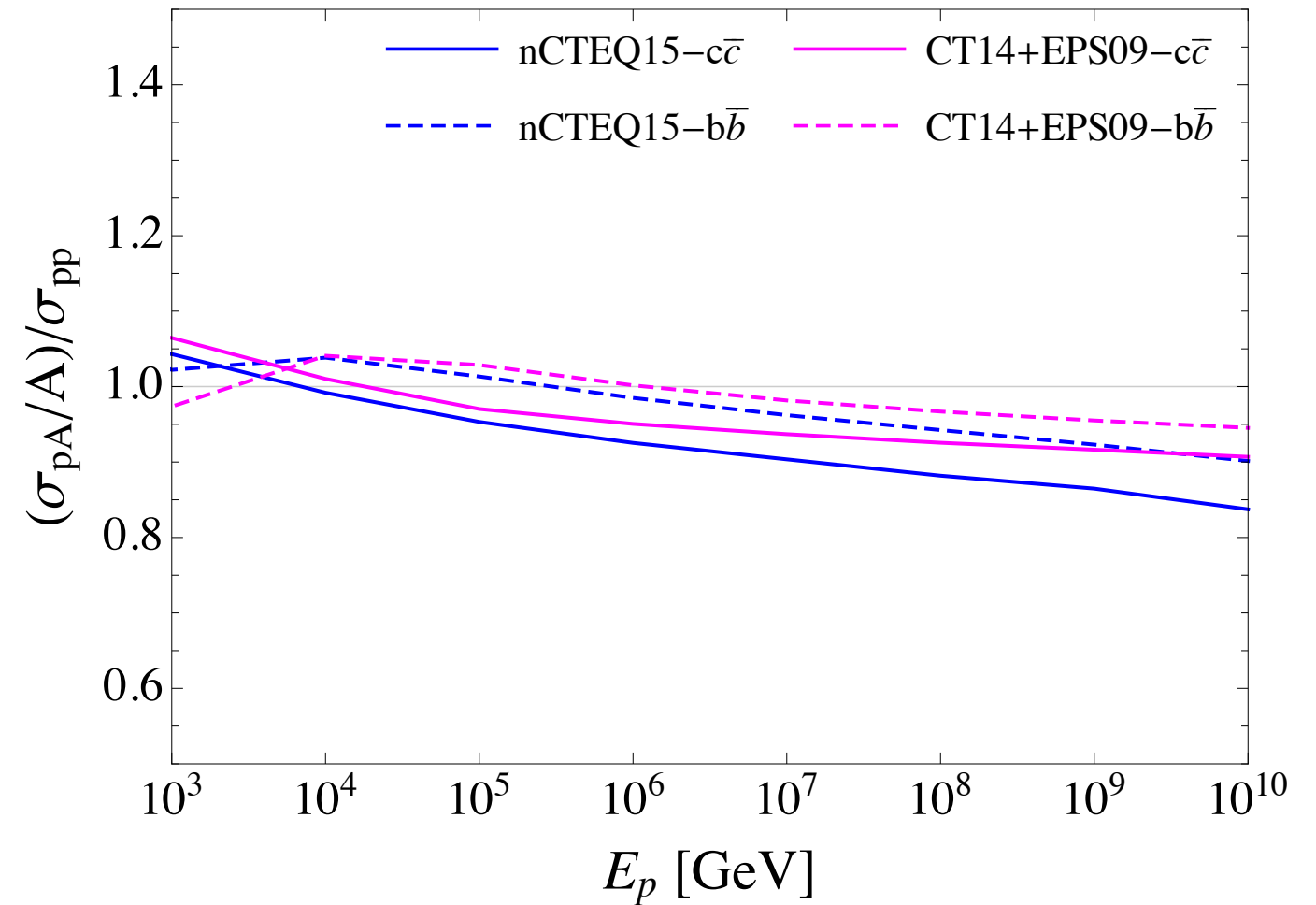
k_T factorization

Small x evolution with the nonlinear density term enhanced by factor proportional to mass number A

Nuclear corrections

Nuclear modifications to the total charm production cross section are small:

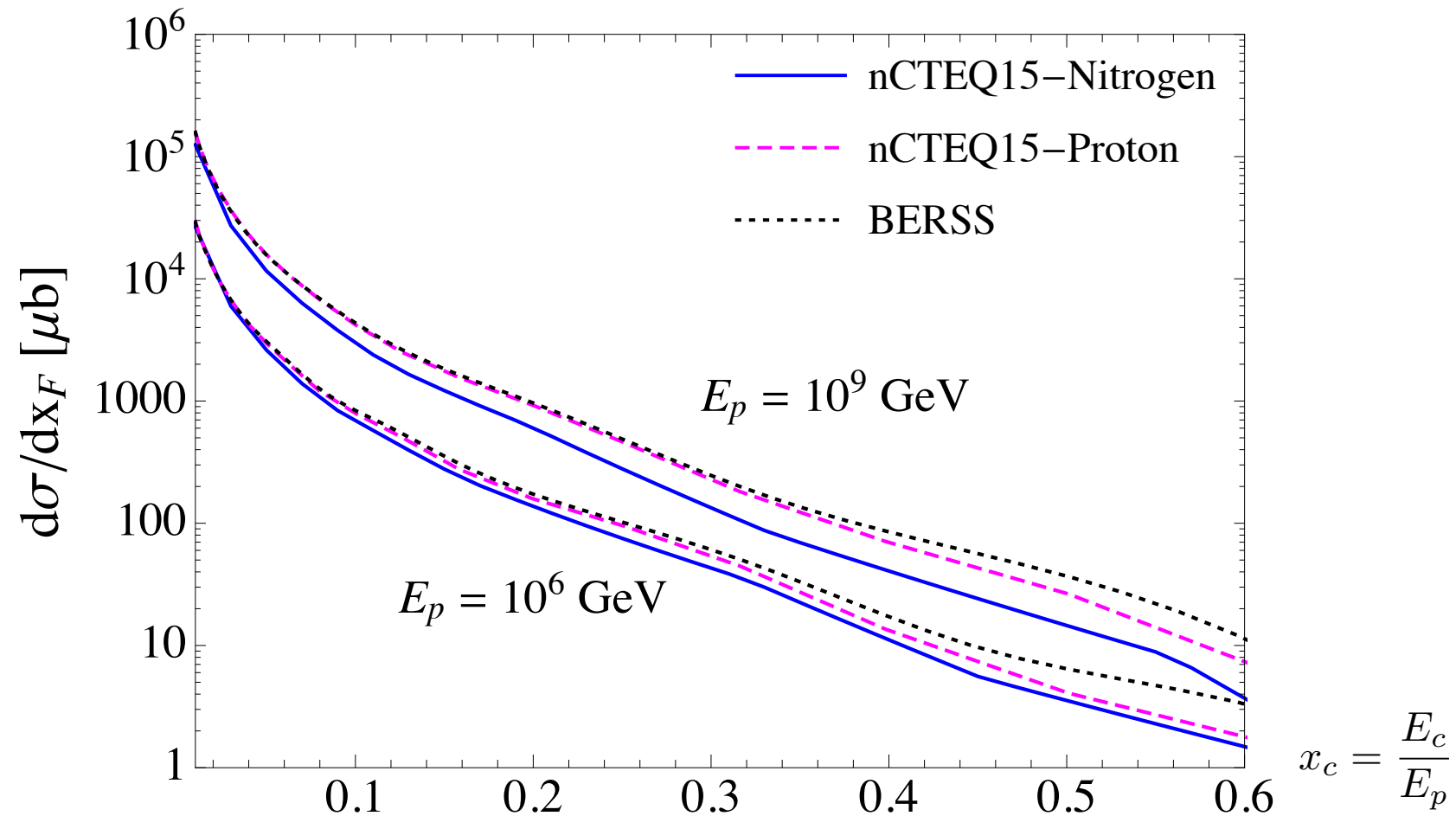
10%-15% for charm
5%-10% for bottom



| E_p | $\sigma(pp \rightarrow c\bar{c}X) [\mu\text{b}]$ | | $\sigma(pA \rightarrow c\bar{c}X)/A [\mu\text{b}]$ | | $[\sigma_{pA}/A]/[\sigma_{pp}]$ | |
|-----------|--|-----------------------|--|-----------------------|---------------------------------|-----------------------|
| | $M_{F,R} \propto m_T$ | $M_{F,R} \propto m_c$ | $M_{F,R} \propto m_T$ | $M_{F,R} \propto m_c$ | $M_{F,R} \propto m_T$ | $M_{F,R} \propto m_c$ |
| 10^2 | 1.51 | 1.87 | 1.64 | 1.99 | 1.09 | 1.06 |
| 10^3 | 3.84×10^1 | 4.72×10^1 | 4.03×10^1 | 4.92×10^1 | 1.05 | 1.04 |
| 10^4 | 2.52×10^2 | 3.06×10^2 | 2.52×10^2 | 3.03×10^2 | 1.00 | 0.99 |
| 10^5 | 8.58×10^2 | 1.03×10^3 | 8.22×10^2 | 9.77×10^2 | 0.96 | 0.95 |
| 10^6 | 2.25×10^3 | 2.63×10^3 | 2.10×10^3 | 2.43×10^3 | 0.93 | 0.92 |
| 10^7 | 5.36×10^3 | 5.92×10^3 | 4.90×10^3 | 5.35×10^3 | 0.91 | 0.90 |
| 10^8 | 1.21×10^4 | 1.23×10^4 | 1.08×10^4 | 1.09×10^4 | 0.89 | 0.89 |
| 10^9 | 2.67×10^4 | 2.44×10^4 | 2.35×10^4 | 2.11×10^4 | 0.88 | 0.86 |
| 10^{10} | 5.66×10^4 | 4.67×10^4 | 4.94×10^4 | 3.91×10^4 | 0.87 | 0.84 |

Differential charm cross section

Differential charm cross section in proton-nucleon collision as a function of the fraction of the incident beam energy carried by the charm quark.

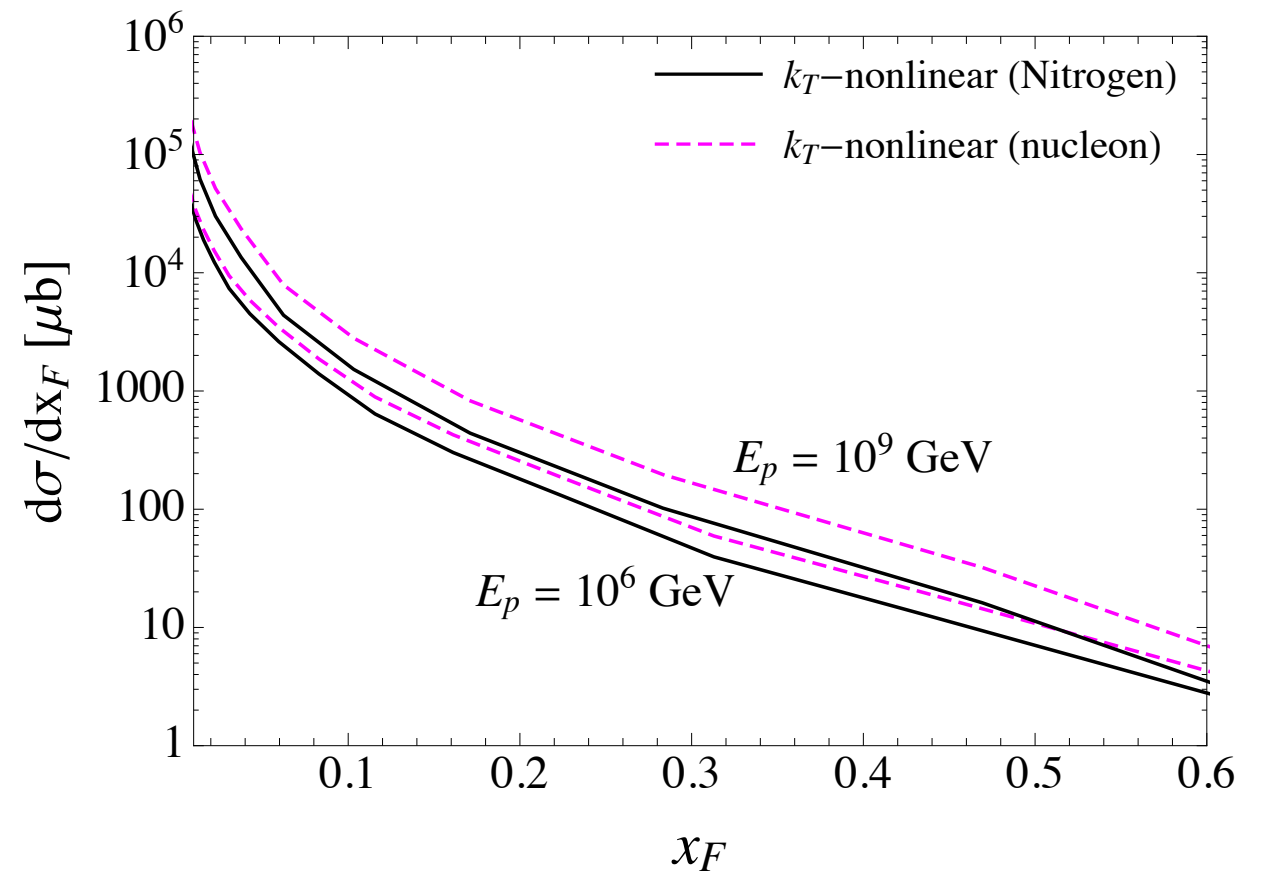
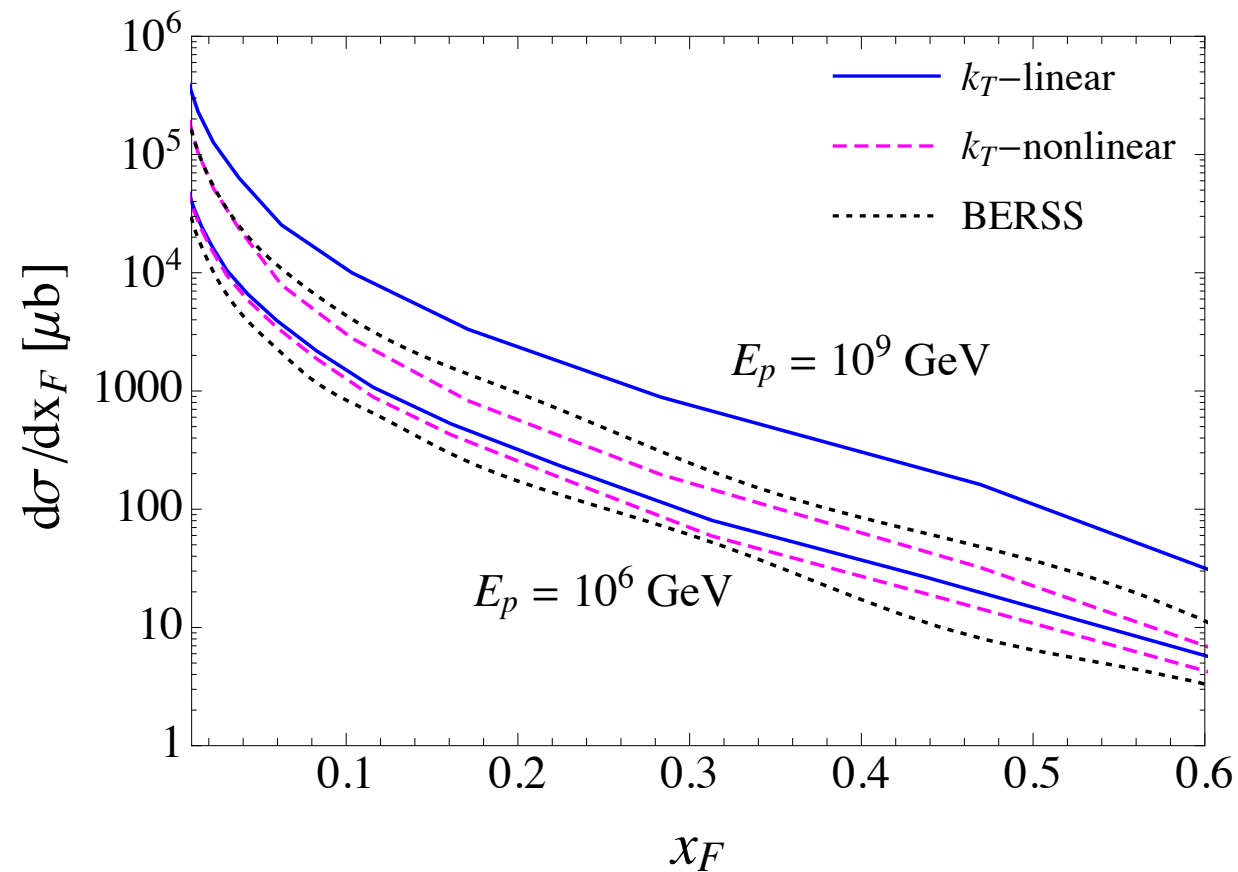


Differential charmed hadron cross section as a function of the energy: need to convolute with the fragmentation function

$$\frac{d\sigma}{dE_h} = \sum_k \int \frac{d\sigma}{dE_k} (AB \rightarrow kX) D_k^h \left(\frac{E_h}{E_k} \right) \frac{dE_k}{E_k} \quad h = D^\pm, D^0(\bar{D}^0), D_s^\pm, \Lambda_c^\pm$$

Using Kniehl, Kramer fragmentation functions.

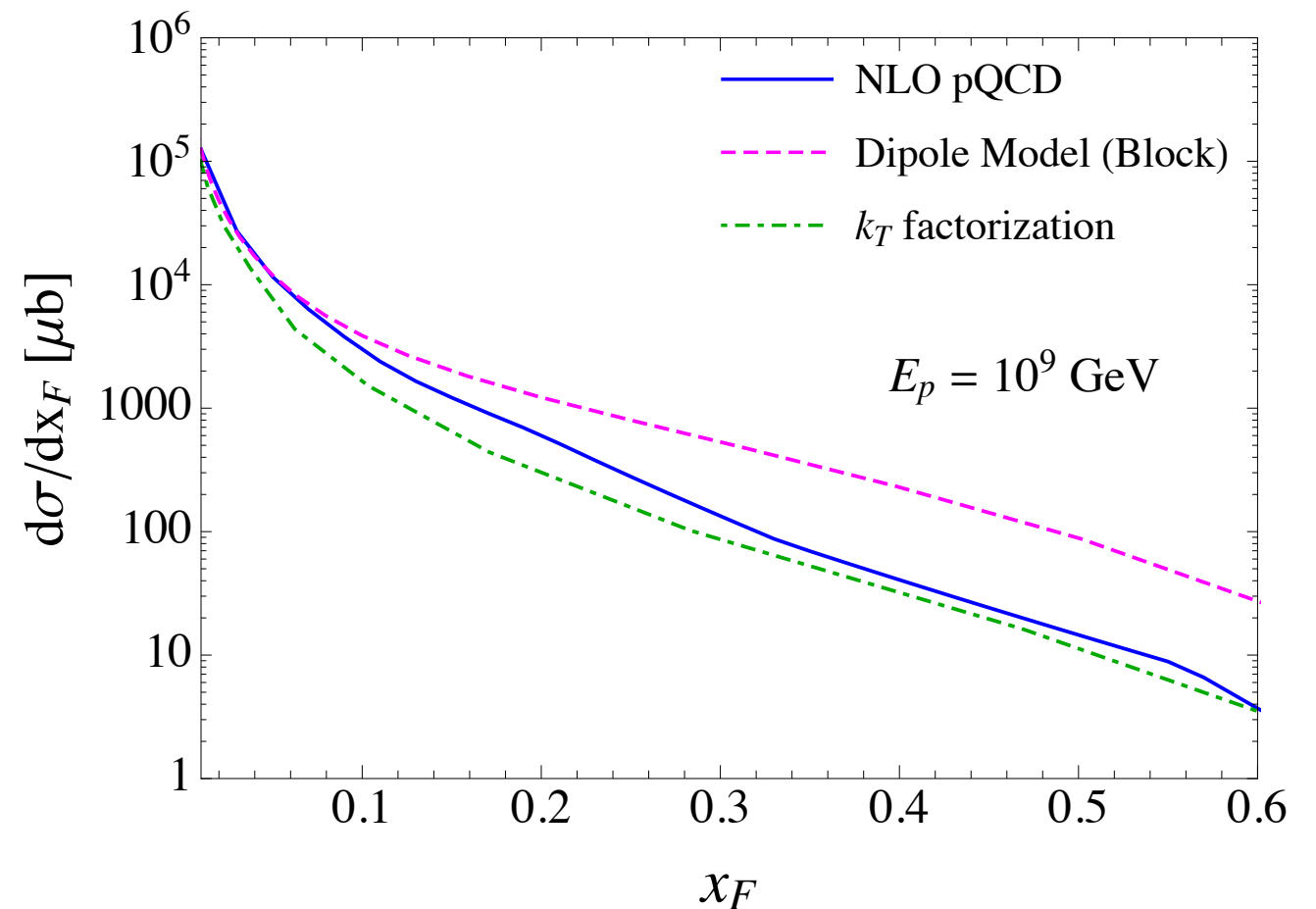
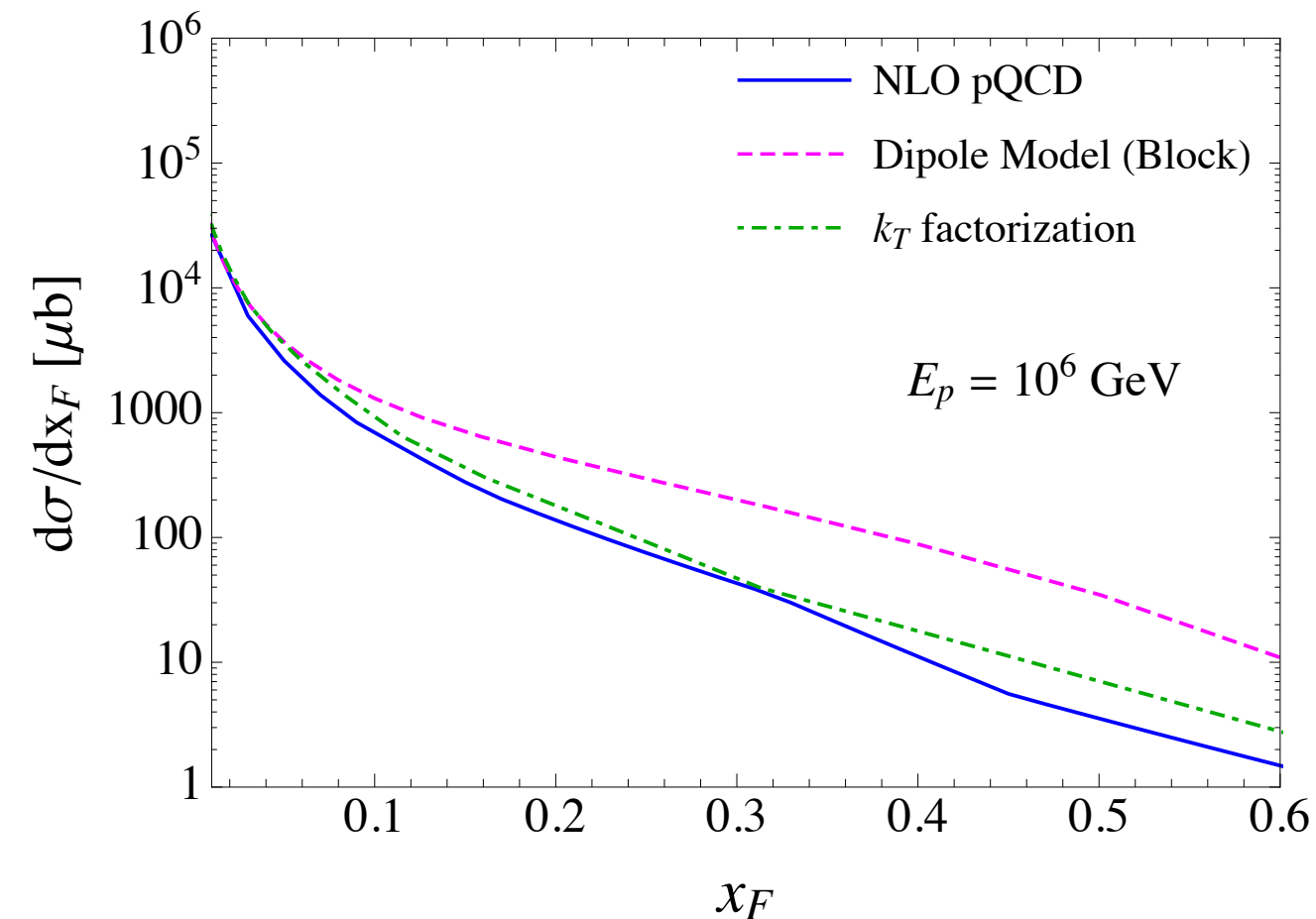
Differential charm cross section



- Parton saturation effects affect the differential cross section more than the integrated cross section.
- Reduction of the cross section, at large energy of the charm quark.
- Nuclear effects in nitrogen are non-negligible at these energies.

Differential charm cross section

Comparison of NLO pQCD, dipole model, and k_T factorization

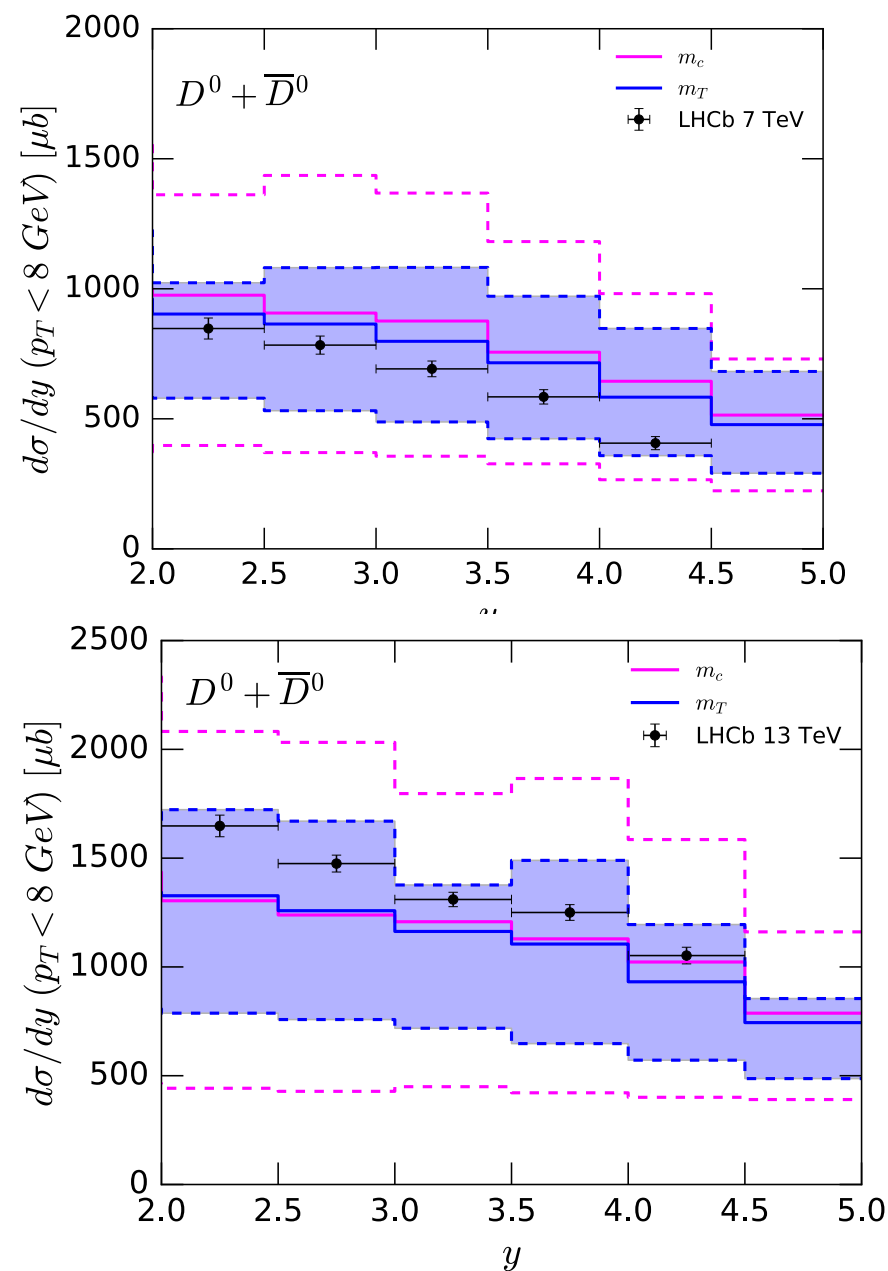


- NLO calculation and k_T factorization calculation consistent with each other.
- Dipole calculation systematically above the other two : need for improvements in this model.

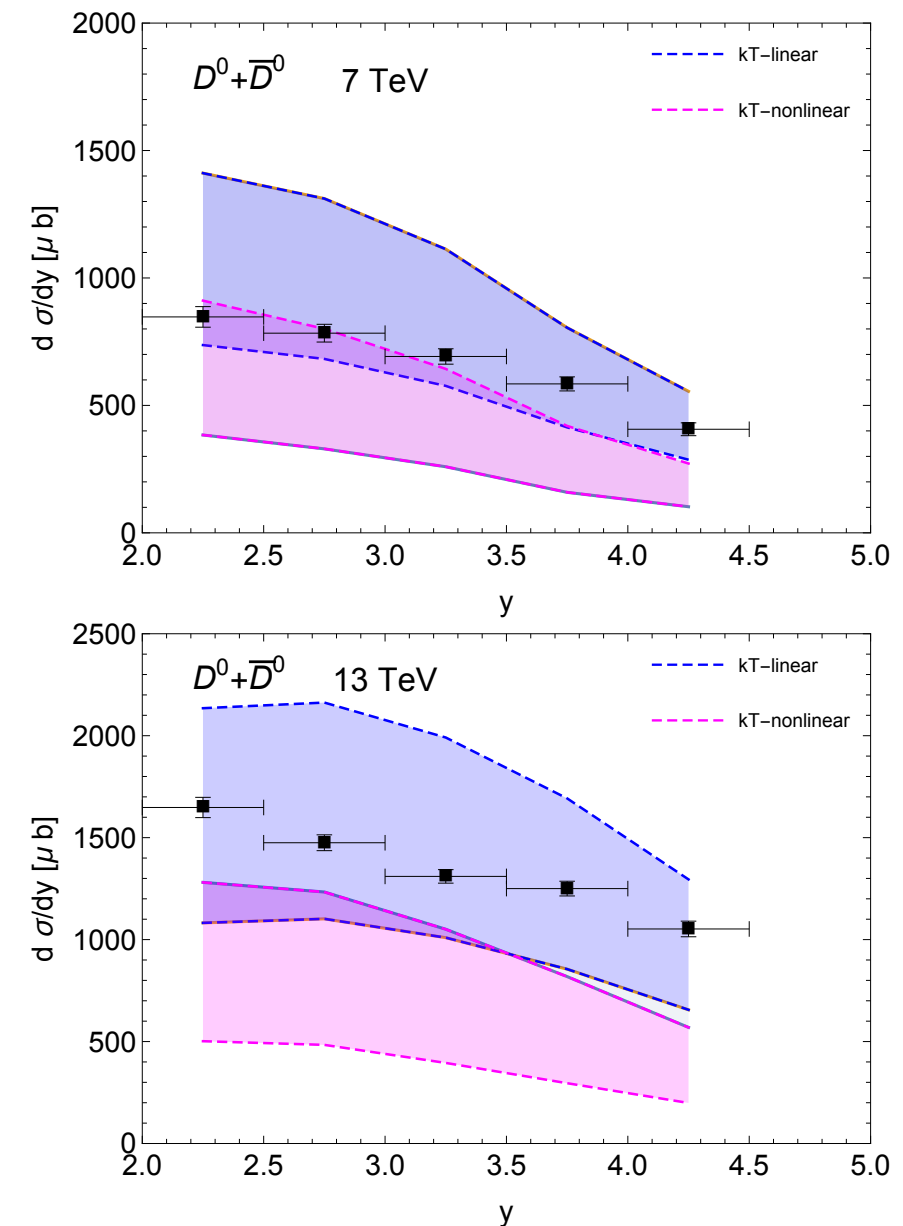
Comparison with LHCb 7 and 13 TeV

Rapidity distributions

NLO collinear



k_T Resummed BFKL+DGLAP

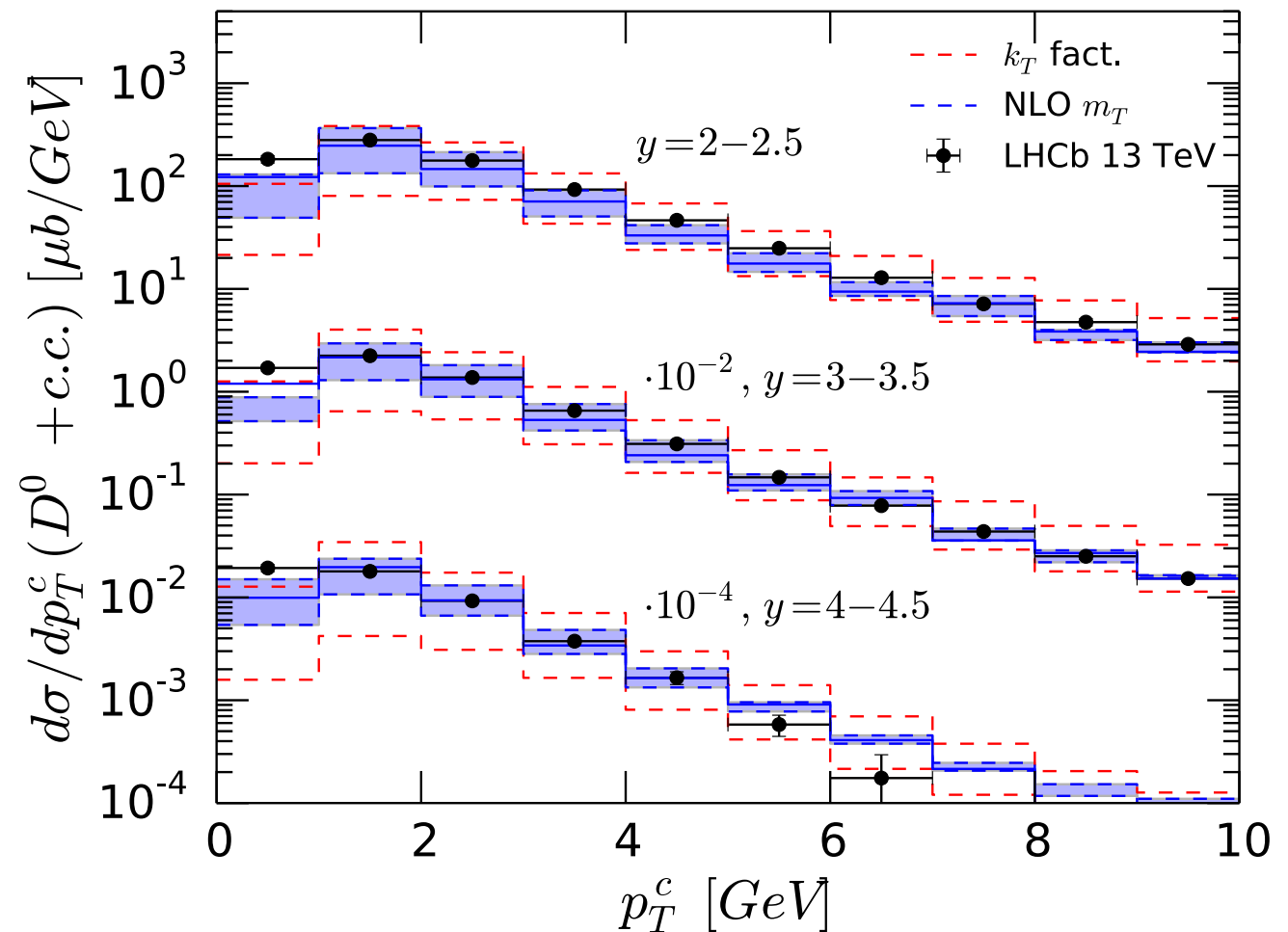
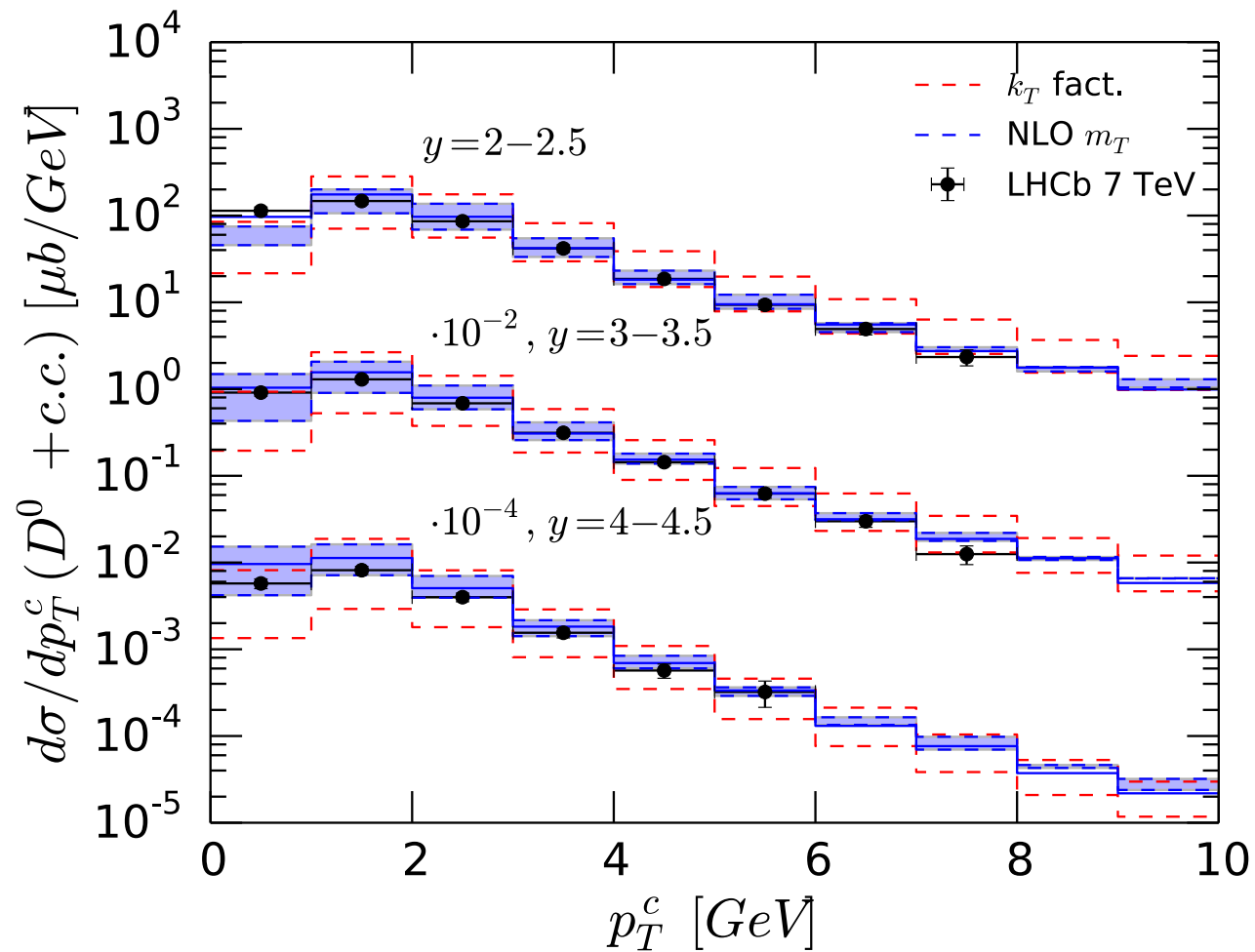


Bands in NLO calculation come from variation of scale : quark mass and transverse mass

Bands in k_T factorization come from varying the upper cutoff on transverse momentum integral between the transverse mass of the quark and maximum value

Comparison with LHCb 7 and 13 TeV

Transverse momentum distributions



- NLO pQCD and k_T factorization consistent with each other.
- Bands on NLO pQCD calculation correspond to scale variation.
- Two lines in k_T factorization correspond to the saturation/no-saturation calculation.

Comparison with LHCb 7 and 13 TeV

Integrated cross section for charm-anticharm production at 7 and 13 TeV.

$$1 < p_T < 8 \text{ GeV}/c$$

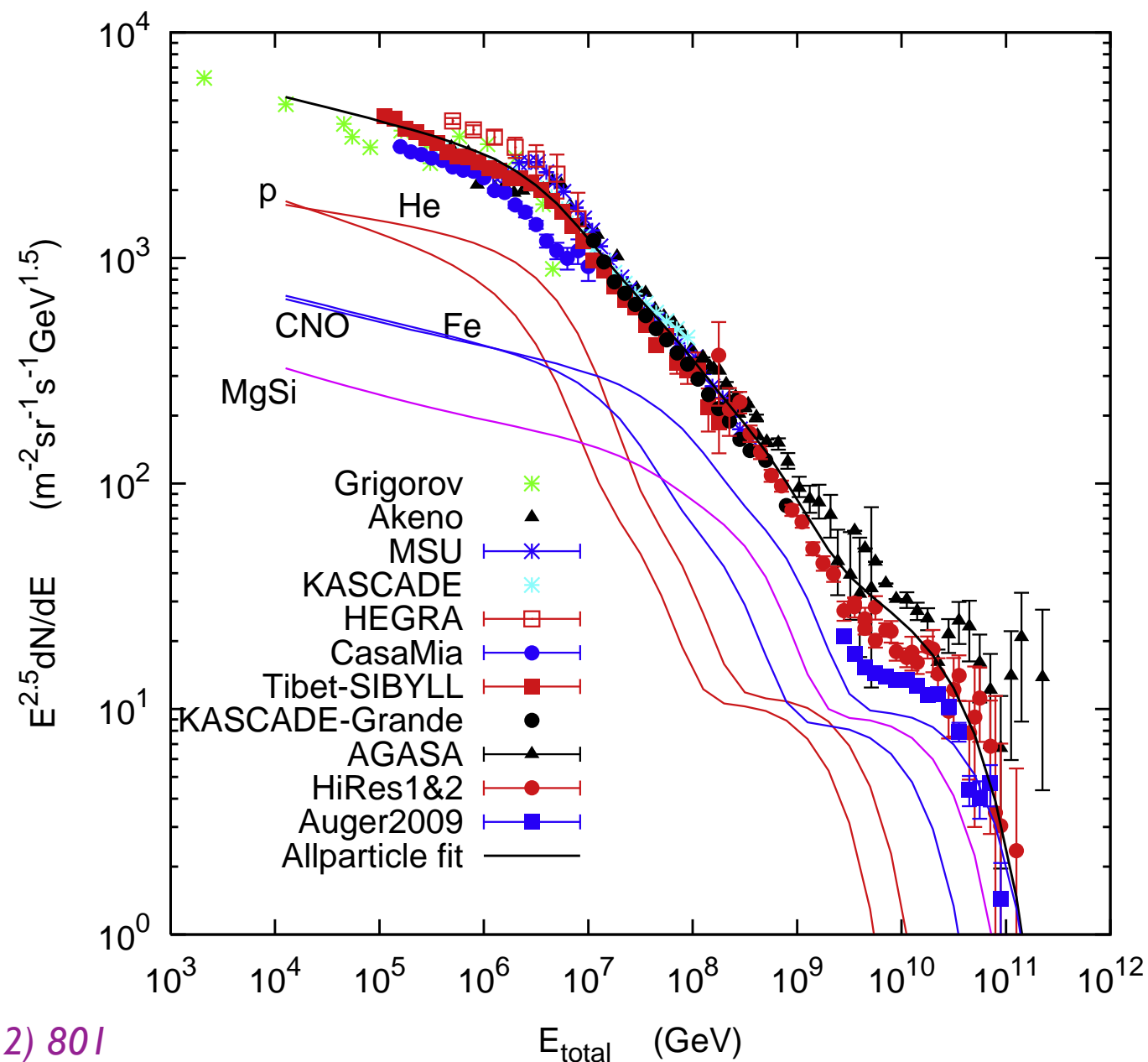
$$2.0 < y < 4.5$$

| \sqrt{s} | $\sigma(pp \rightarrow c\bar{c}X) [\mu\text{b}]$ | | | | |
|------------|--|---------------------------|------------------------|------------------|----------------|
| | NLO ($\mu \propto m_T$) | NLO ($\mu \propto m_c$) | DM | k_T | Experiment |
| 7 TeV | 1610^{+480}_{-620} | 1730^{+900}_{-1020} | 1619^{+726}_{-705} | $1347 \div 1961$ | 1419 ± 134 |
| 13 TeV | 2410^{+700}_{-960} | 2460^{+1440}_{-1560} | 2395^{+1276}_{-1176} | $2191 \div 3722$ | 2369 ± 192 |

Cosmic ray flux

Important ingredient for lepton fluxes: initial cosmic ray flux.

Parametrization by Gaisser (2012) with three populations and five nuclei groups:
H, He, CNO, Fe, MgSi



Gaisser,

Astroparticle Physics 35 (2012) 801

Cosmic ray flux

Multicomponent parametrization by Gaisser (2012) with three populations:

1st population: supernova remnants

2nd population: higher energy galactic component

3rd population: extragalactic component

$$\phi_i(E) = \sum_{j=1}^3 a_{ij} E^{-\gamma_{ij}} \times \exp \left[-\frac{E}{Z_i R_{c,j}} \right]$$

$a_{i,j}$ normalization

$\gamma_{i,j}$ spectral index

$R_{c,j}$ magnetic rigidity

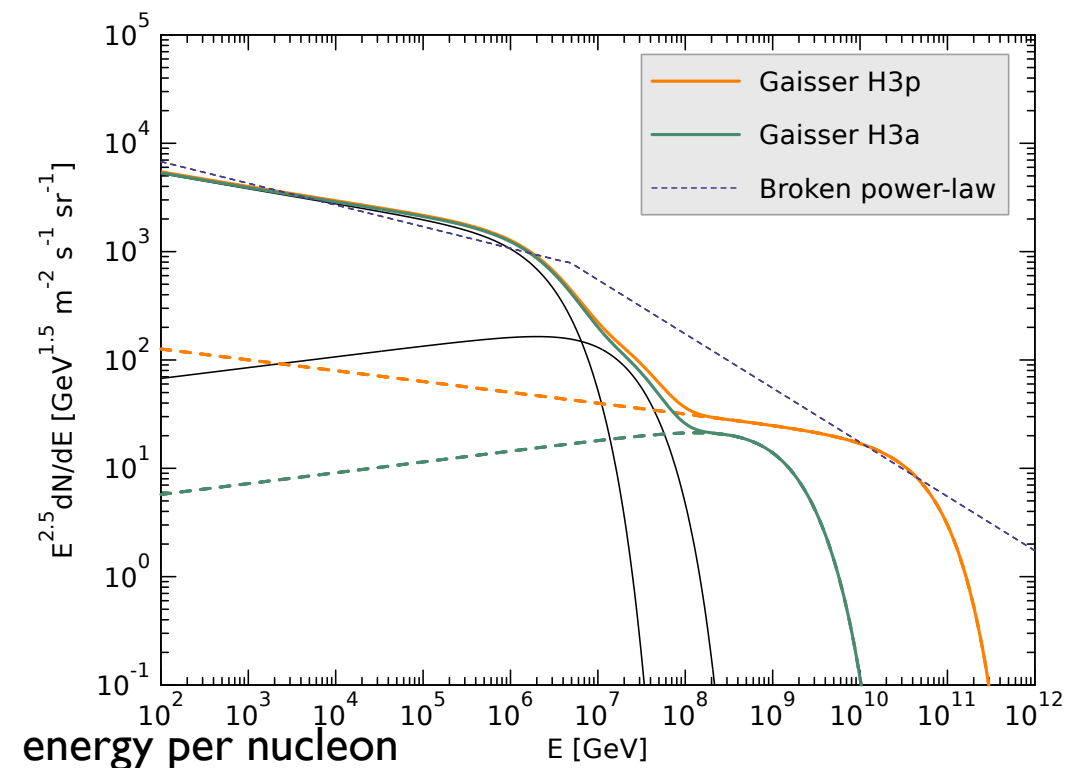
$$E_{\text{tot}}^c = Ze \times R_c$$

$$\phi = dN/d \ln E$$

Converting to nucleon spectrum

$$\phi_{i,N}(E_N) = A \times \phi_i(AE_N)$$

for each component



This power law was used widely in previous evaluations of the prompt neutrino flux

$$\phi_p^0(E) = \begin{cases} 1.7 E^{-2.7} & \text{for } E < 5 \cdot 10^6 \text{ GeV} \\ 174 E^{-3} & \text{for } E > 5 \cdot 10^6 \text{ GeV}, \end{cases}$$

Development of air shower: cascade equations

Production of prompt neutrinos:



where $\text{M} = D^\pm, D^0, D_s, \Lambda_c$

Use set of cascade equations in **depth X**

$$X = \int_h^\infty \rho(h') dh'$$

$$\frac{d\Phi_j}{dX} = -\frac{\Phi_j}{\lambda_j} - \frac{\Phi_j}{\lambda_j^{dec}} + \sum_k \int_E^\infty dE_k \frac{\Phi_k(E_k, X)}{\lambda_k(E_k)} \frac{dn_{k \rightarrow j}(E; E_k)}{dE}$$

λ_j interaction length and $\lambda_j^{dec} = \gamma c \tau_j \rho(X)$ decay length

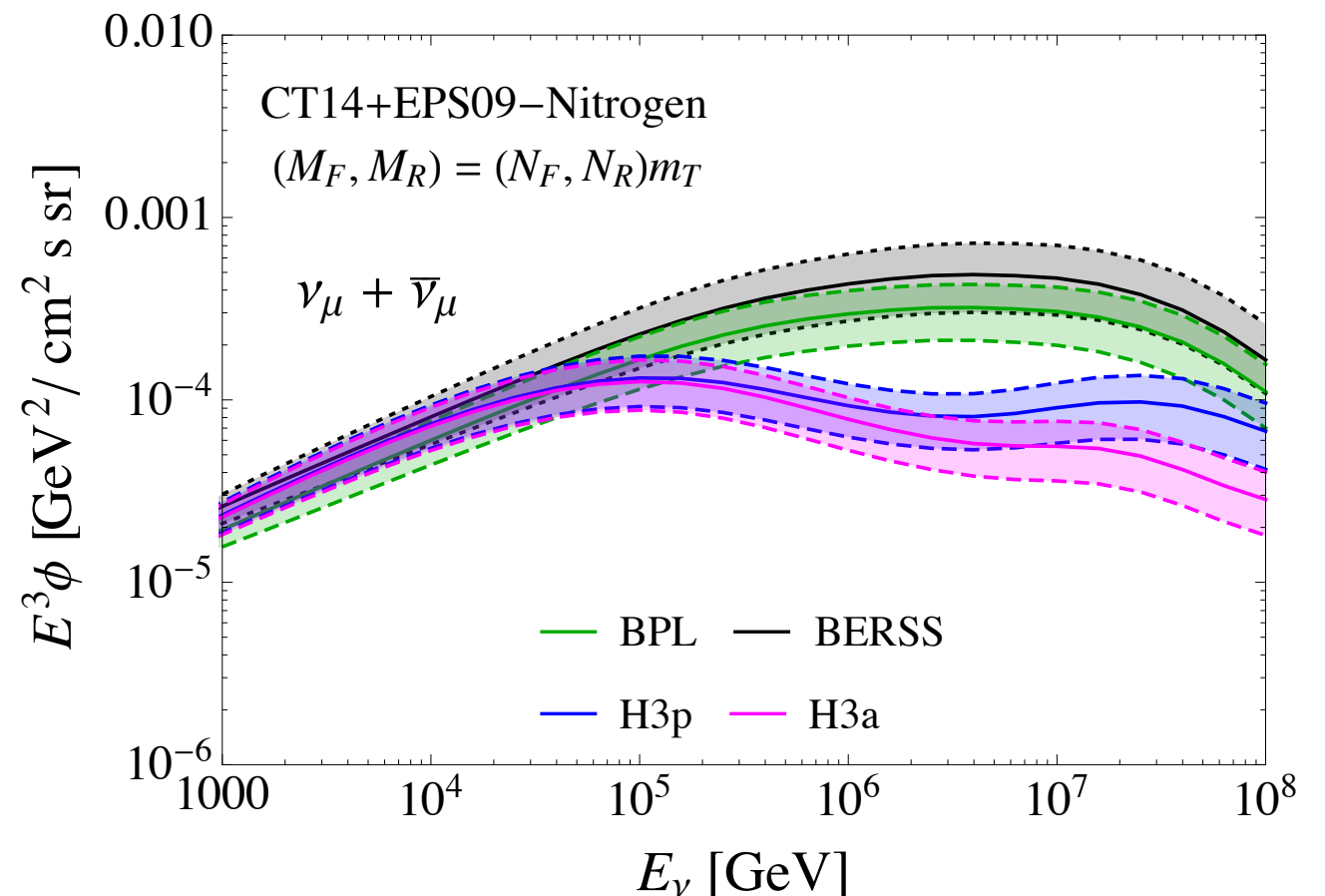
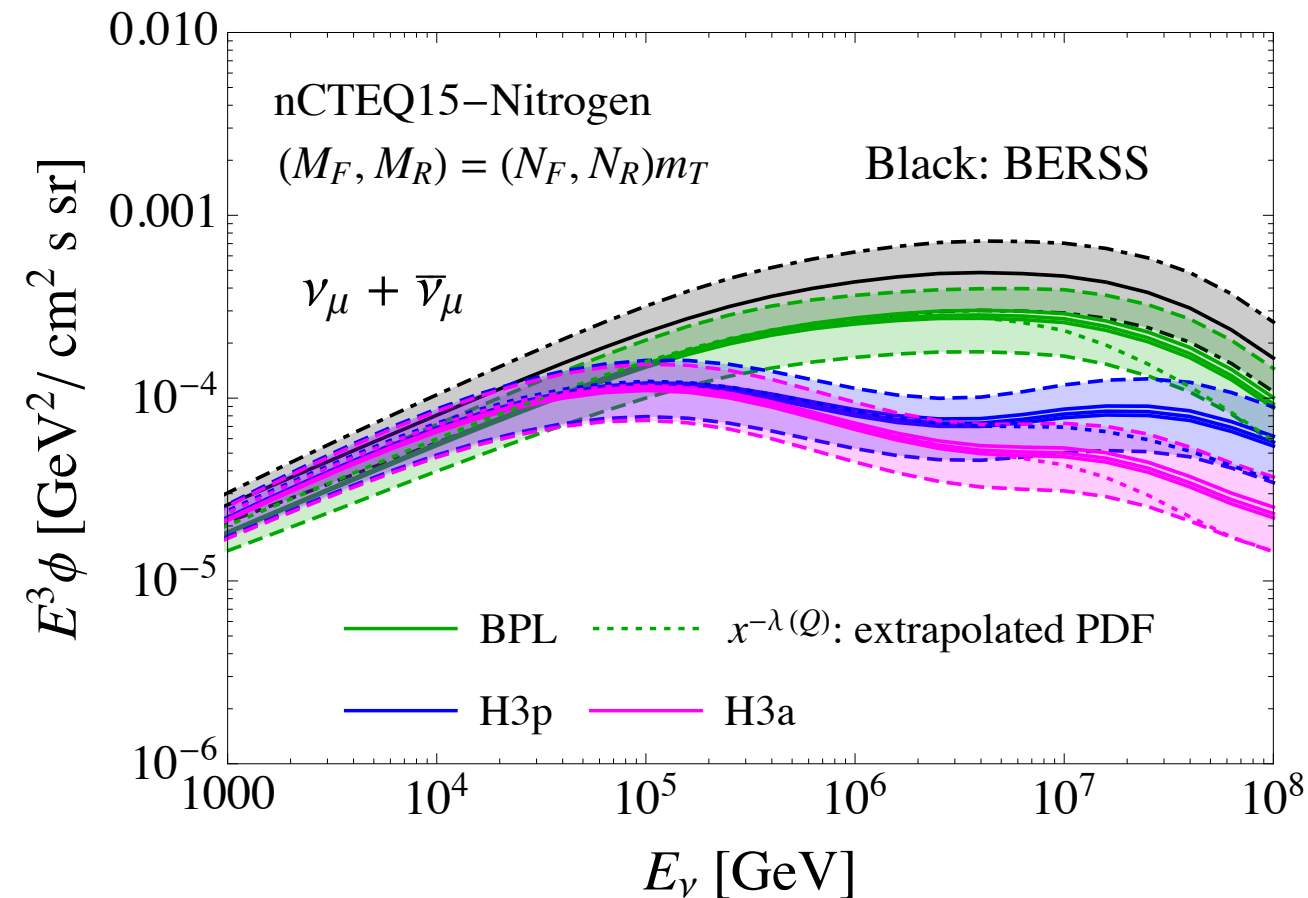
$\frac{dn_{k \rightarrow j}}{dE}$ production or decay distribution

$$\frac{1}{\sigma_k} \frac{d\sigma_{k \rightarrow j}(E, E_k)}{dE} \qquad \frac{1}{\Gamma_k} \frac{d\Gamma_{k \rightarrow j}(E, E_k)}{dE}$$

Need to solve these equations simultaneously assuming non-zero initial proton flux.

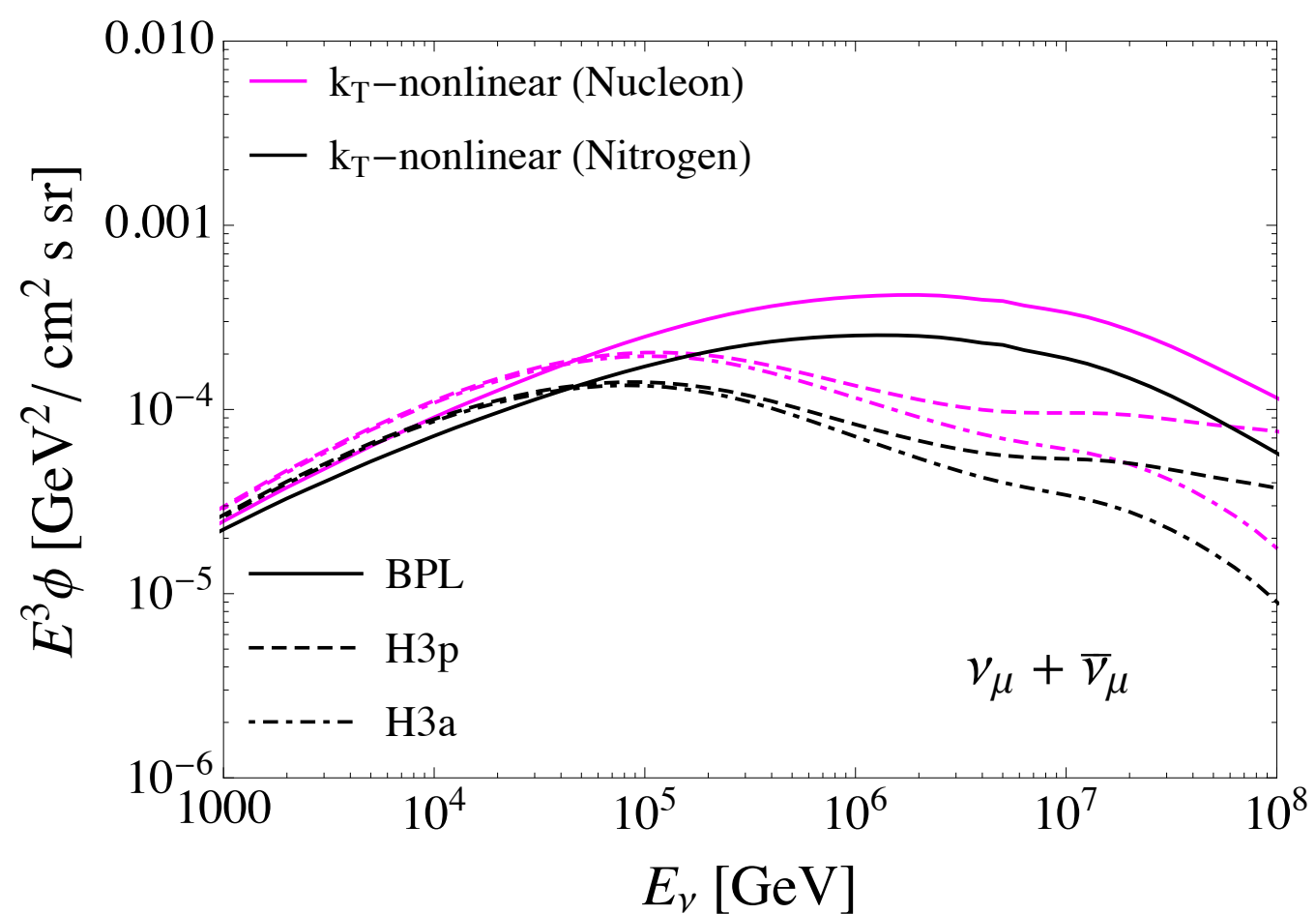
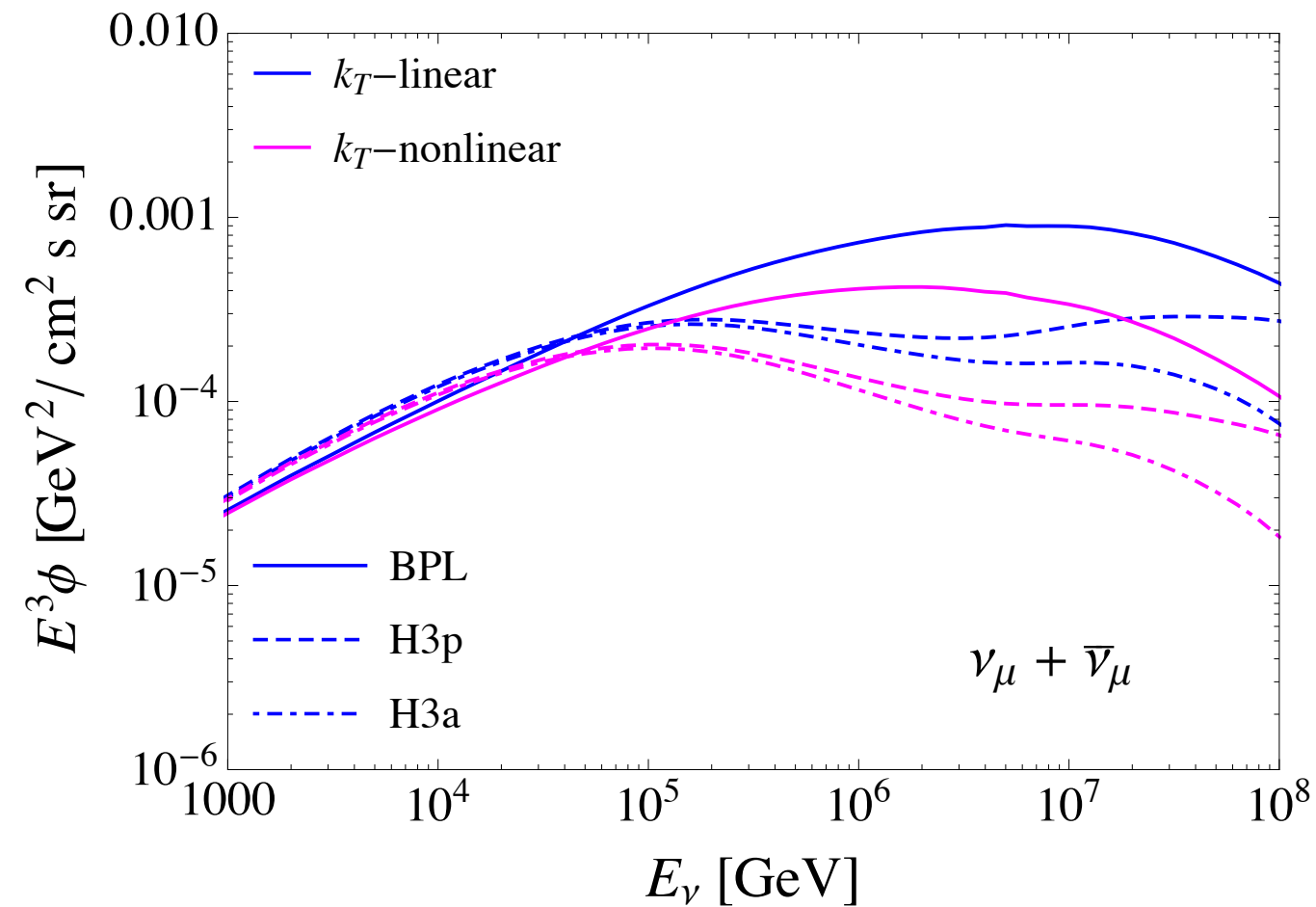
Neutrino fluxes

flux of $\nu_\mu + \bar{\nu}_\mu$



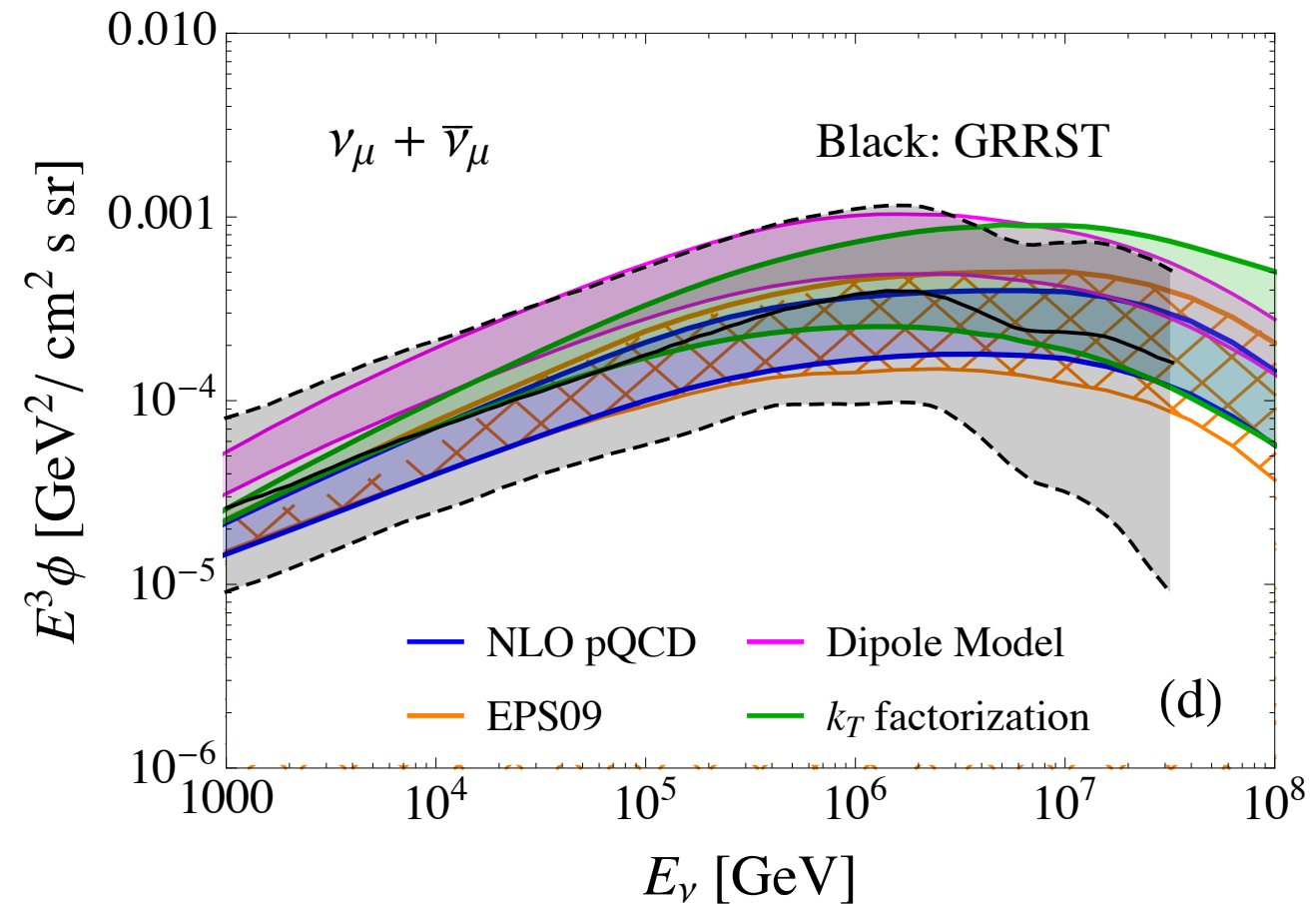
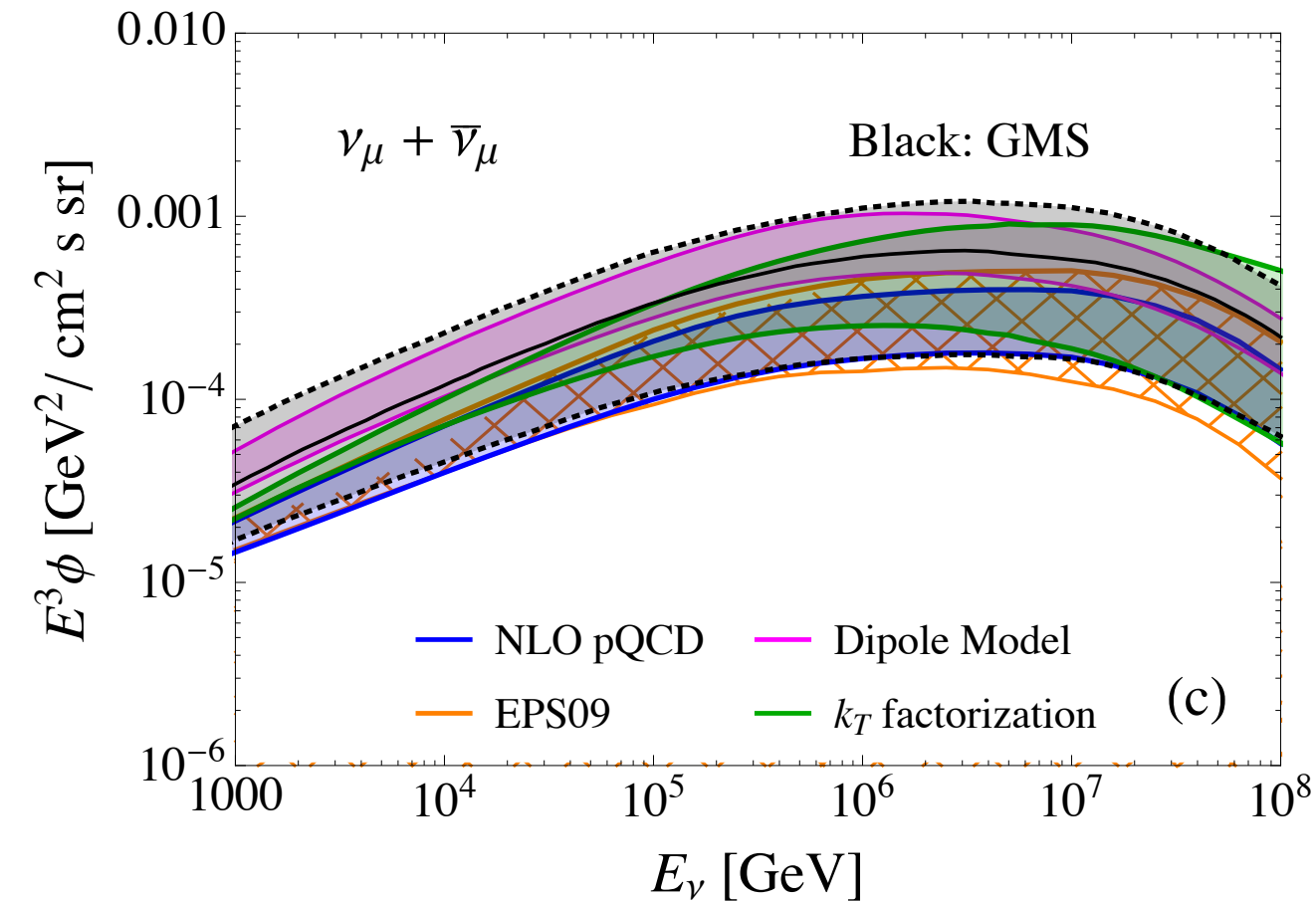
- Significant reduction (factor 2-3) due to the updated cosmic ray spectrum with respect to the broken power law.
- The reduction is in the region of interest, where prompt neutrino component should dominate over the atmospheric one.
- Black band: previous calculation.
- The updated fragmentation function reduces flux by 20%.
- B hadron contribution increases flux by about 5-10%.
- Nuclear effects: 20-35%.
- Combined effects: reduction by 45% at highest energies.

Neutrino fluxes



- Sizeable reduction of the flux due to the changes from linear to nonlinear evolution in k_T factorization.
- Further reduction of the flux when nuclear effects in nitrogen are included.

Neutrino fluxes



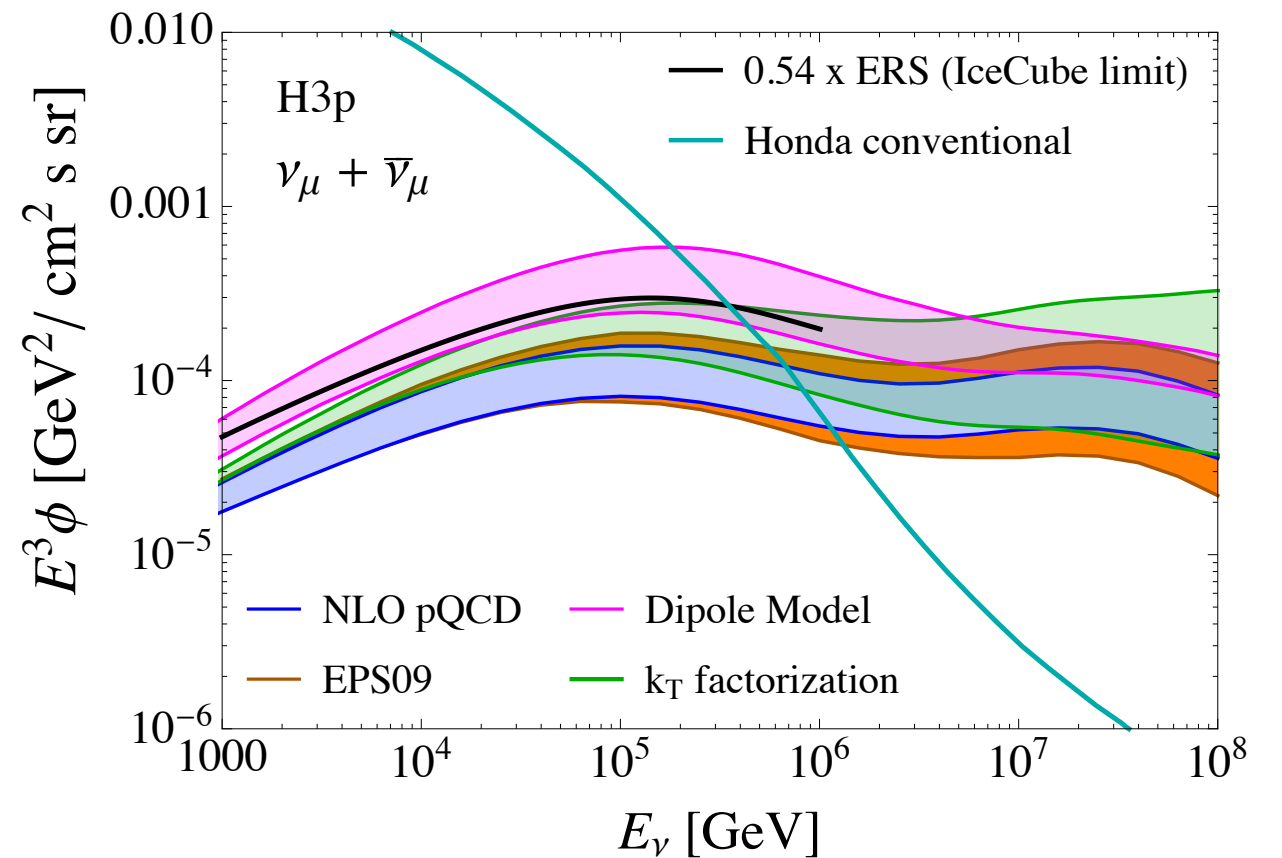
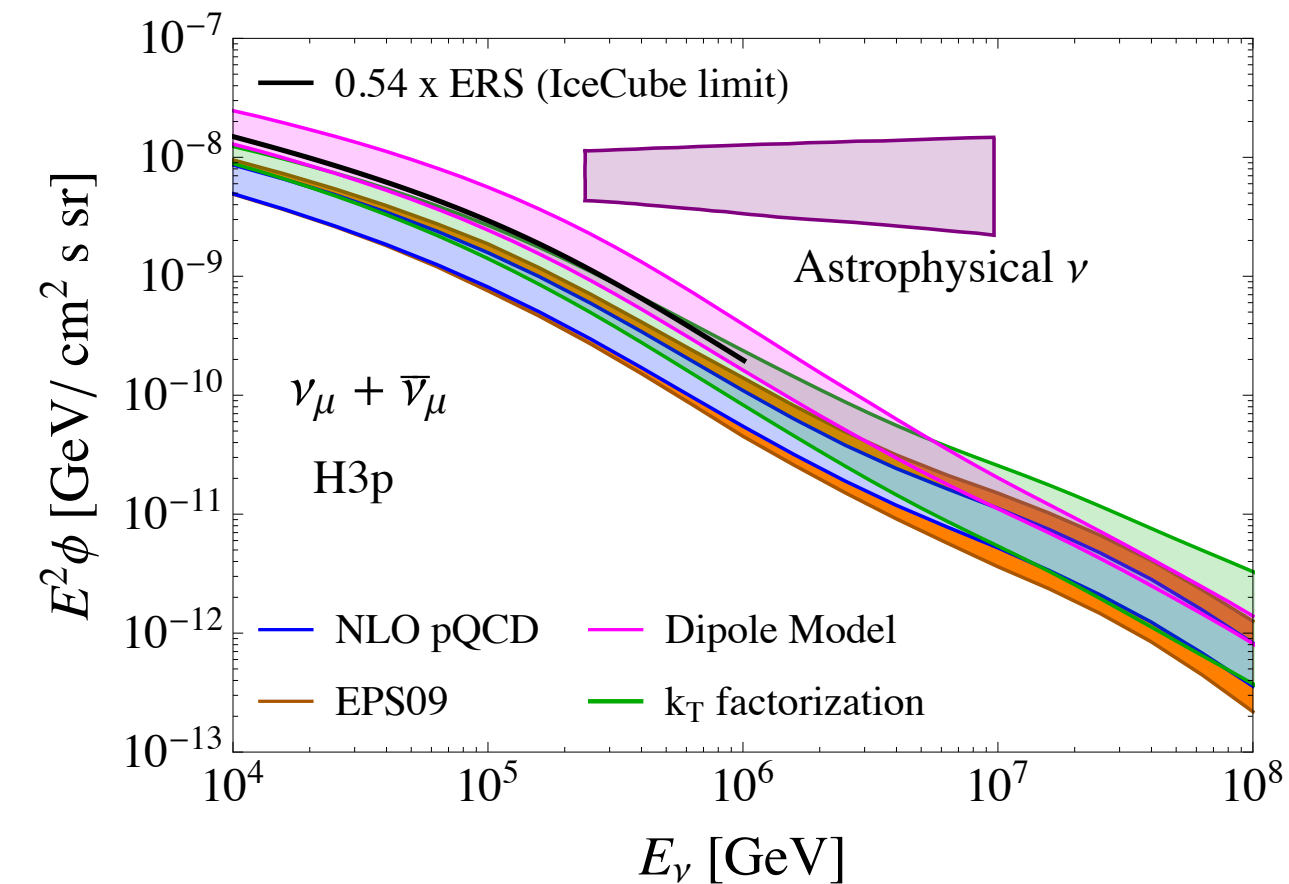
Comparison with other calculations:

GMS: Garzelli, Moch, Sigl

GRRST: Gauld, Rojo, Rotoli, Sarkar, Talbert

Consistency within the error bands.

Predictions and IceCube limit



- IceCube limit on prompt neutrino flux (PoS(ICRC2015)1079).
- NLO perturbative and k_T factorization within the limit.
- Dipole model calculation is in slight tension with the IceCube limit.
- Overall the flux is well below the astrophysical flux measured by IceCube.

Summary and outlook

- Calculation of the prompt neutrino flux using NLO and new PDFs. Charm cross section matched to LHC and RHIC data. Consistent with LHCb data on forward charm production.
- Updated cosmic ray flux gives lower values (as compared with earlier ERS and BERSS evaluation) for the atmospheric neutrino flux.
- Prompt neutrino component is rather small. The data are significantly above, new calculation can change the evaluation of the statistical significance of the astrophysical signal for IC.
- Nuclear effects in the target. Further reduction of the flux by about 20-35%. Estimate of nuclear corrections within the NLO pQCD consistent with the small x calculation.
- Alternative calculations: dipole and k_T factorization. Small x resummation leads to enhancement, saturation to the reduction of the flux. Dipole model larger than other calculations at low energies, needs improvement.
- Other calculations also on the market: consistent but still large uncertainties. Largest uncertainties due to the QCD scale variation, PDF uncertainties and CR flux.
- Outstanding questions: fragmentation (forward production, hadronic-nuclear environment, differences between PYTHIA and fragmentation functions, recent measurements by LHCb); intrinsic charm.

Backup

Neutrino cross sections

$$\frac{d^2\sigma^{CC}}{dxdy} = \frac{2G_F^2 M_N E_\nu}{\pi} \left(\frac{M_W^2}{Q^2 + M_W^2} \right)^2 \cdot [xq(x, Q^2) + x\bar{q}(x, Q^2)(1-y)^2]$$

$xq(x, Q^2)$, $x\bar{q}(x, Q^2)$ are parton densities.

Since $xq(x, Q^2) \sim x^{-\lambda}$ this implies that

$$\sigma(E_\nu) = \int dxdy \frac{d^2\sigma^{CC}}{dxdy} \sim E_\nu^\lambda$$

Need extrapolations of parton densities to very small x

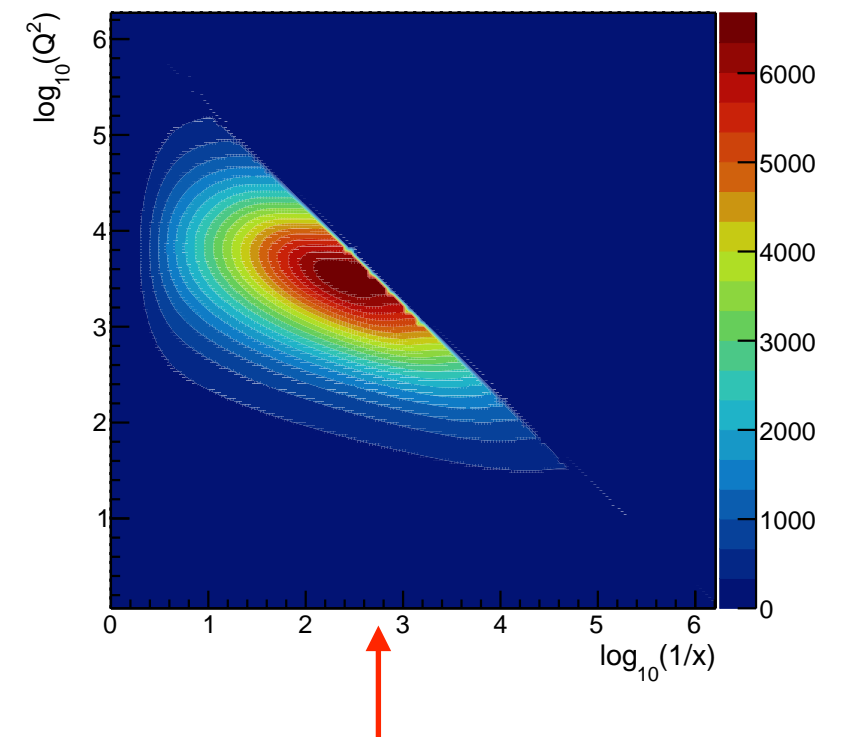
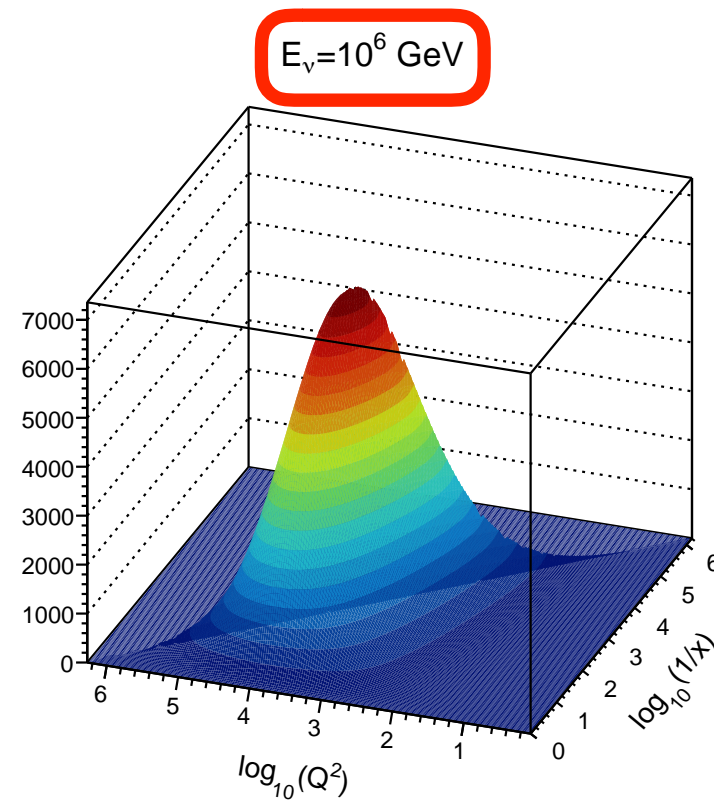
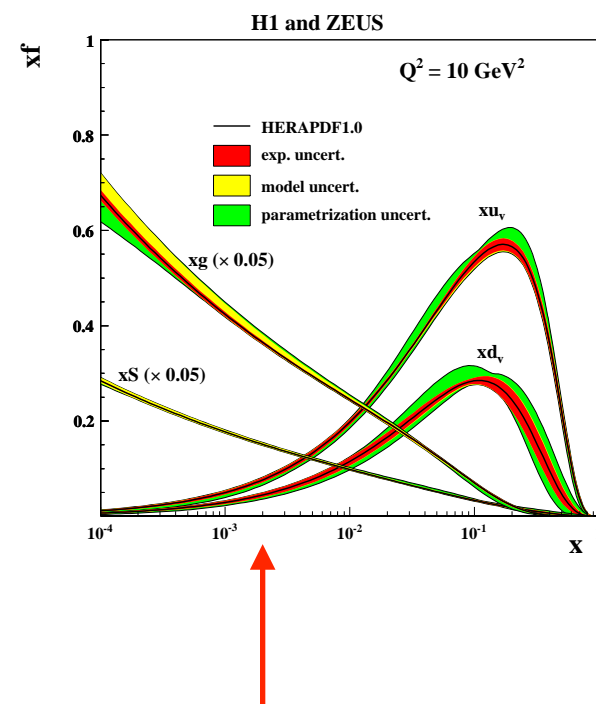
Ghandi, Quigg, Reno, Sarcevic

Neutrino cross sections

Neutrino cross sections

Contribution to the cross section in Q and x plane:

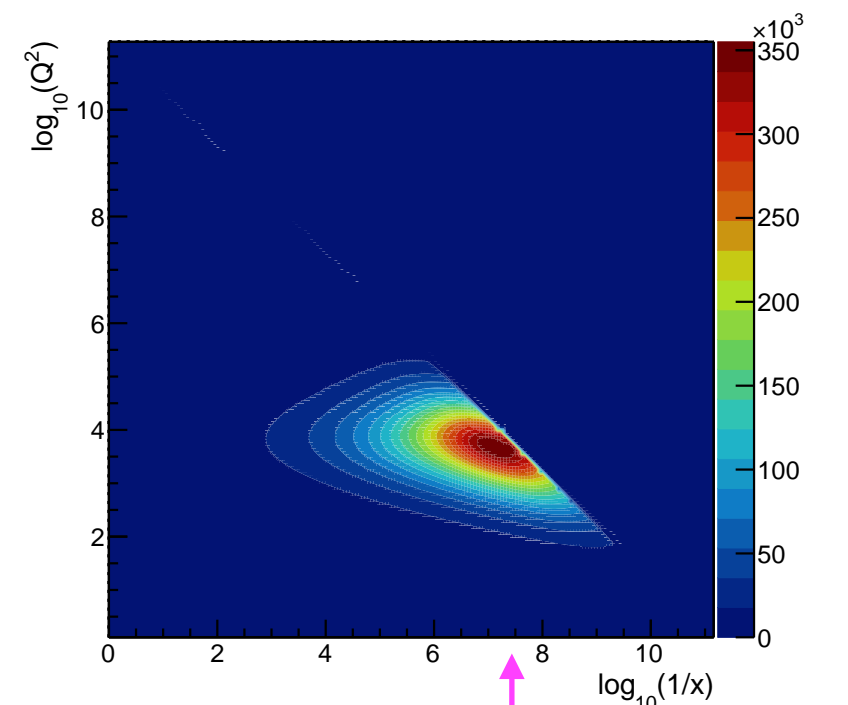
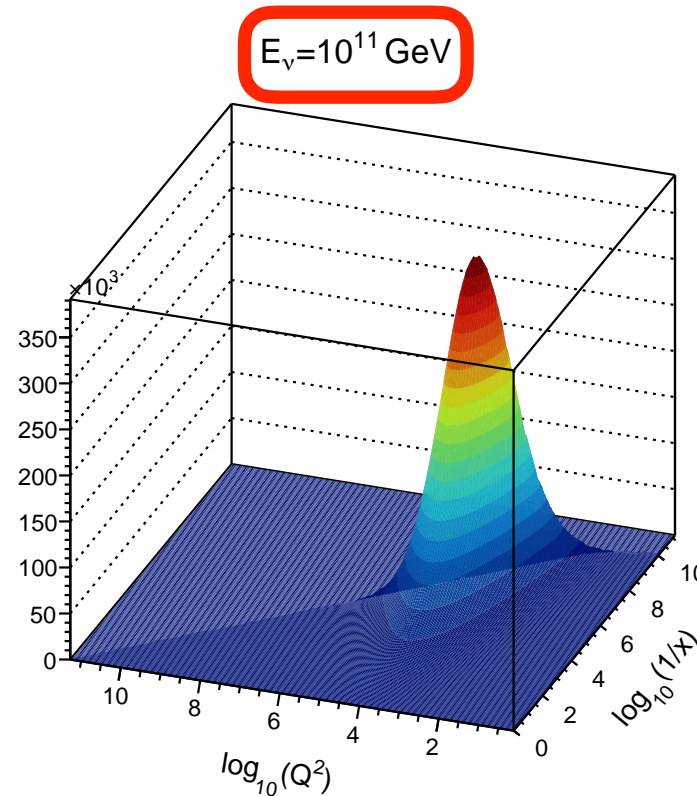
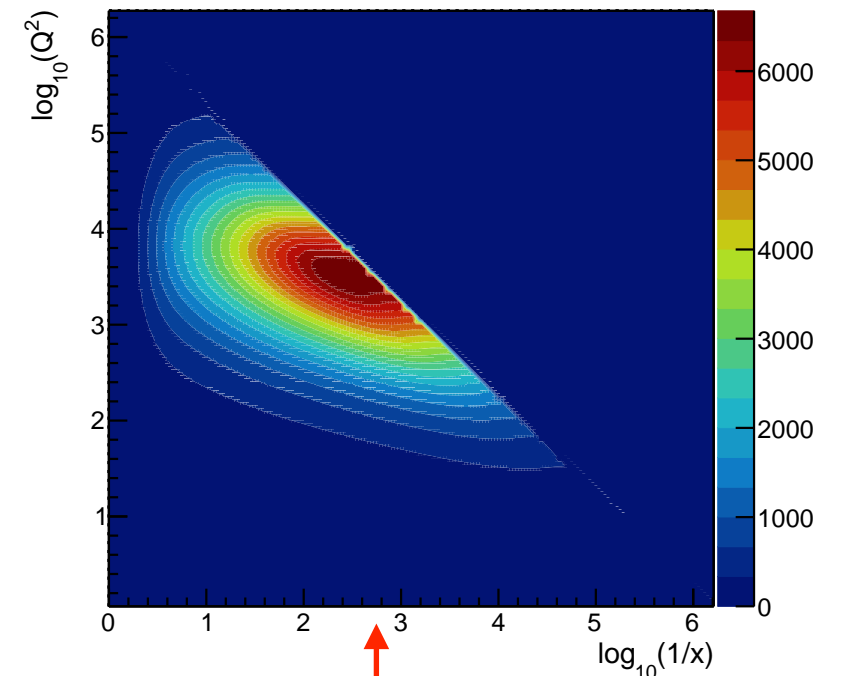
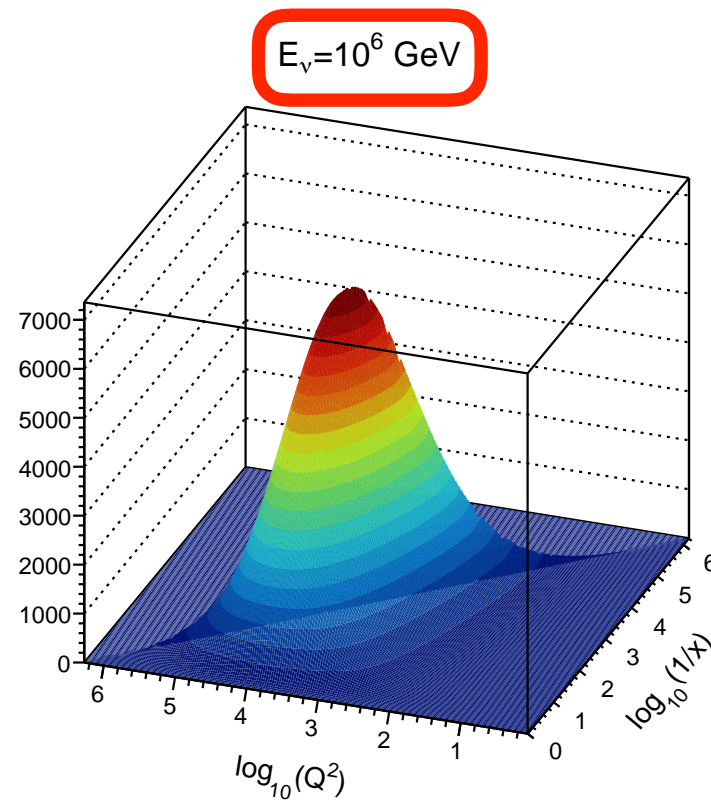
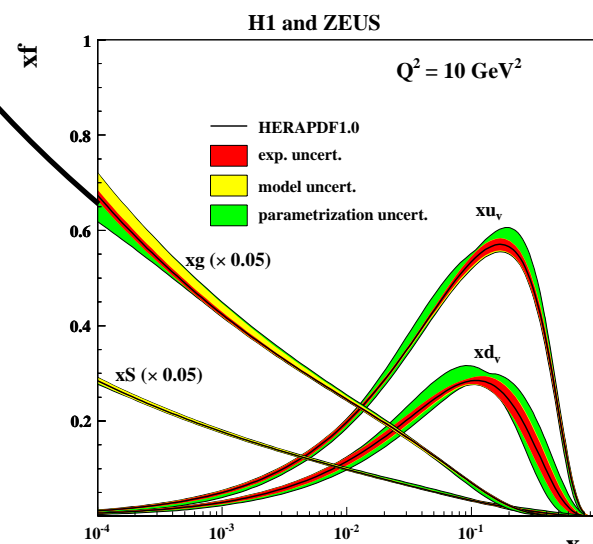
$$xQ^2 \frac{d^2\sigma}{dx dQ^2}$$



Neutrino cross sections

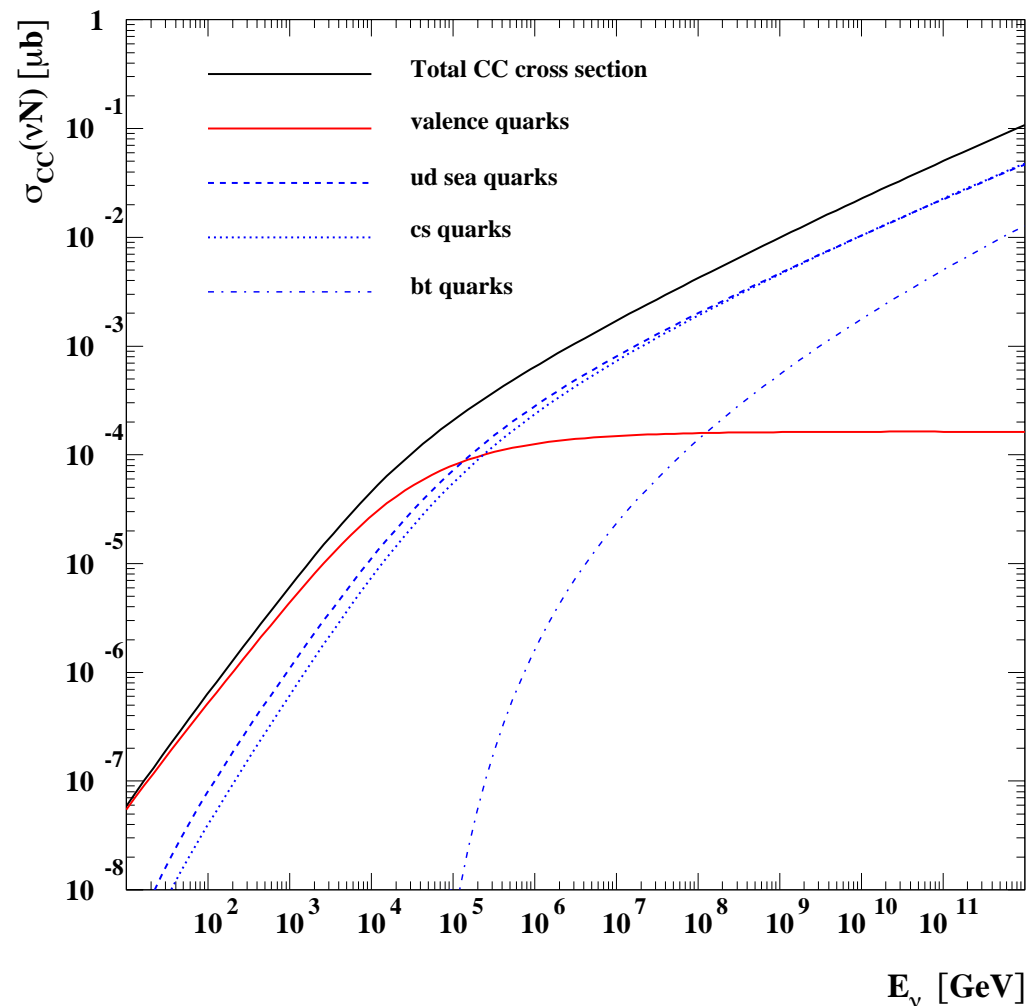
Contribution to the cross section in Q and x plane:

$$xQ^2 \frac{d^2\sigma}{dx dQ^2}$$



Neutrino cross sections

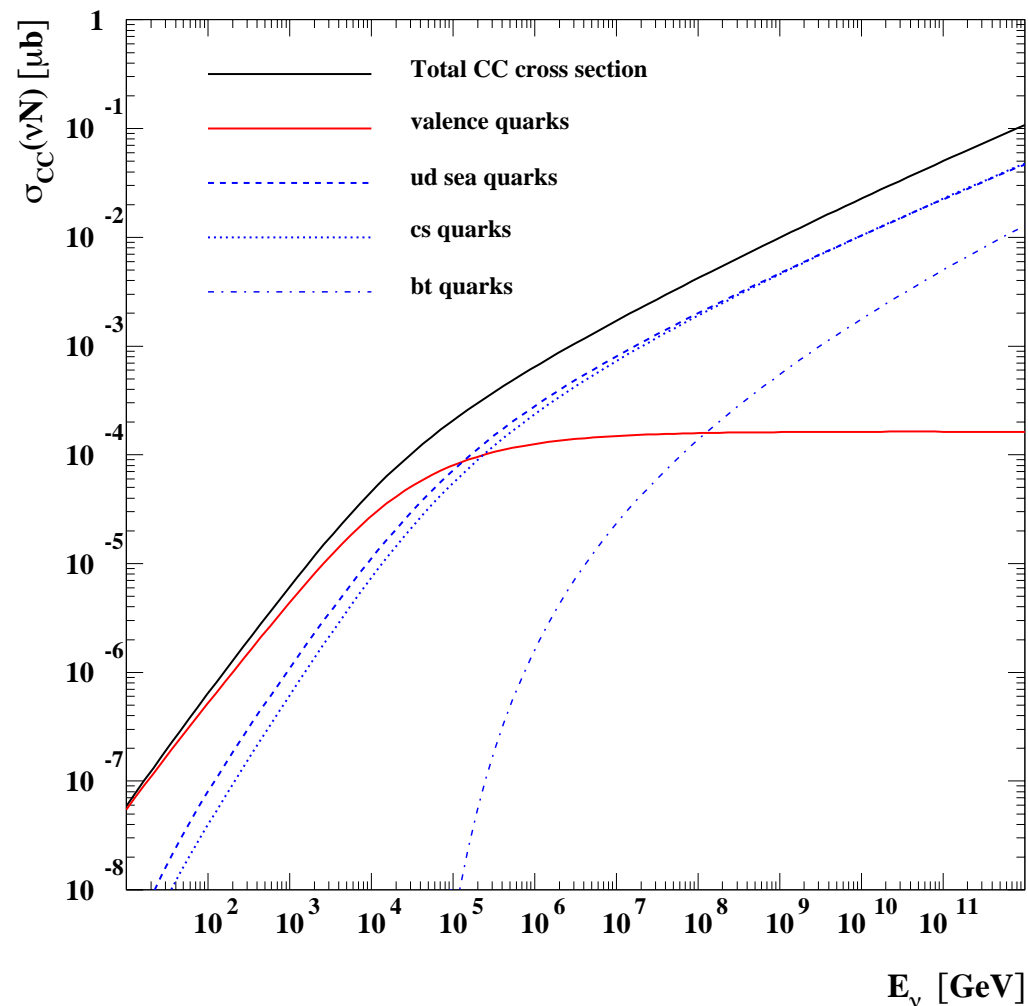
Kwiecinski, Martin, AS



Calculation of the neutrino cross section using unified DGLAP/BFKL evolution: including small x resummation effects.

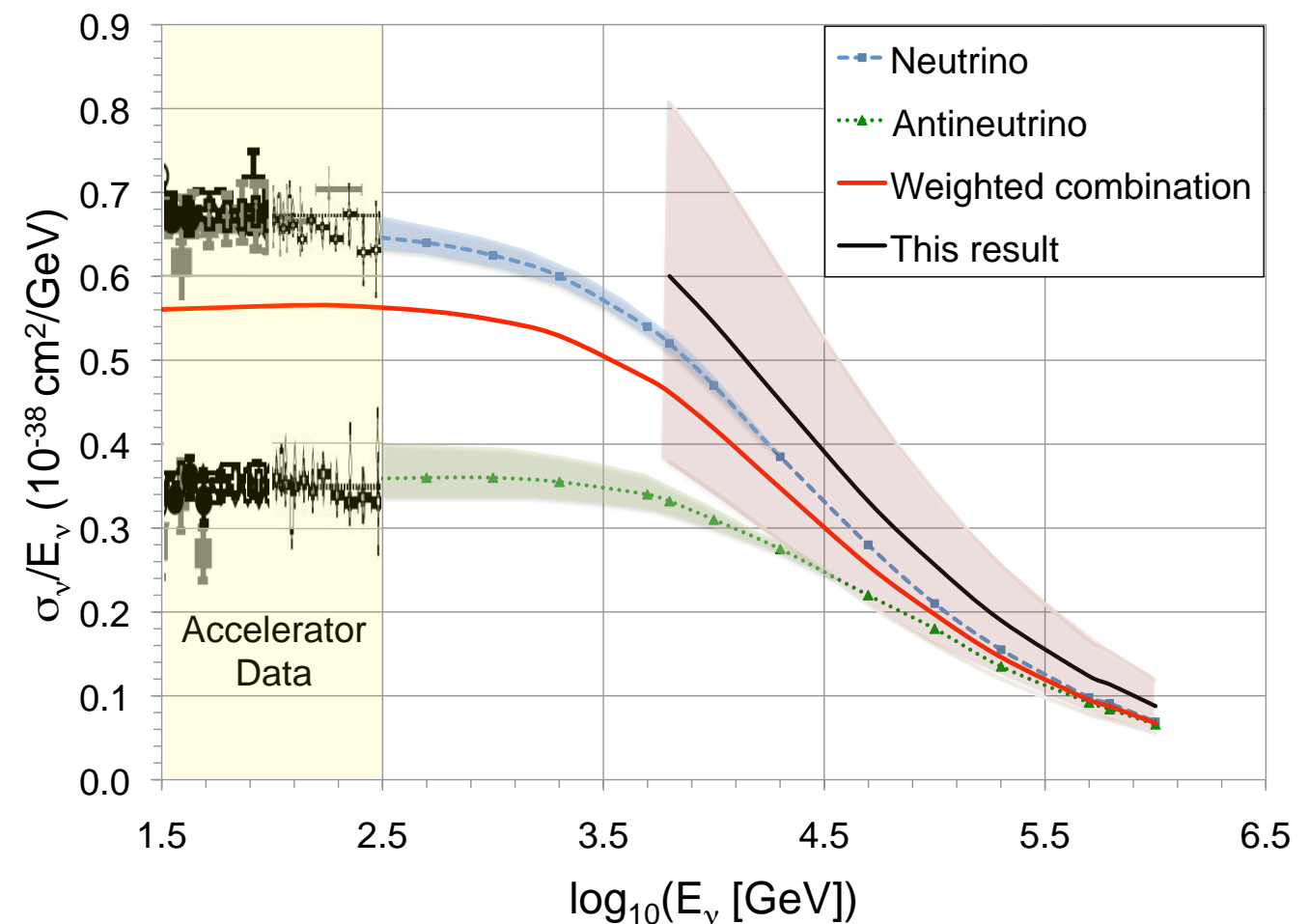
Neutrino cross sections

Kwiecinski, Martin, AS



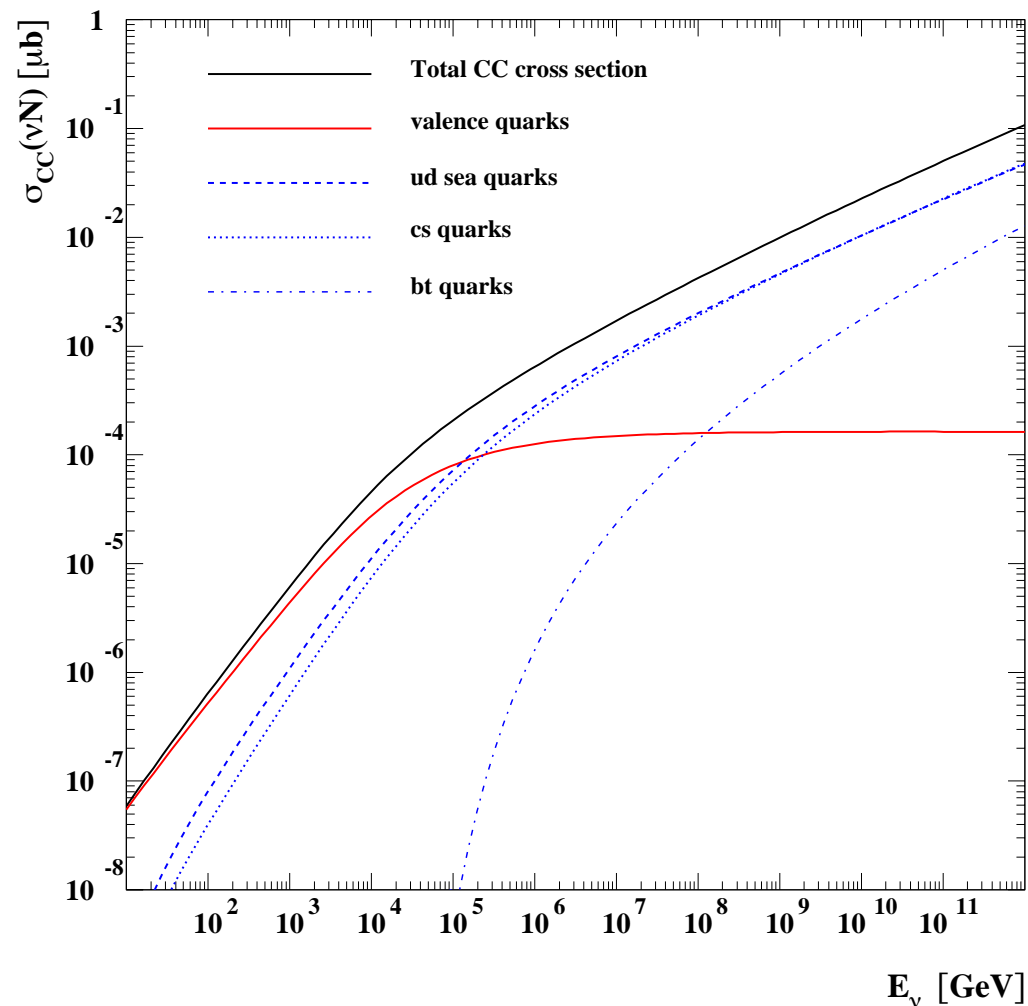
Calculation of the neutrino cross section using unified DGLAP/BFKL evolution: including small x resummation effects.

ICECUBE result



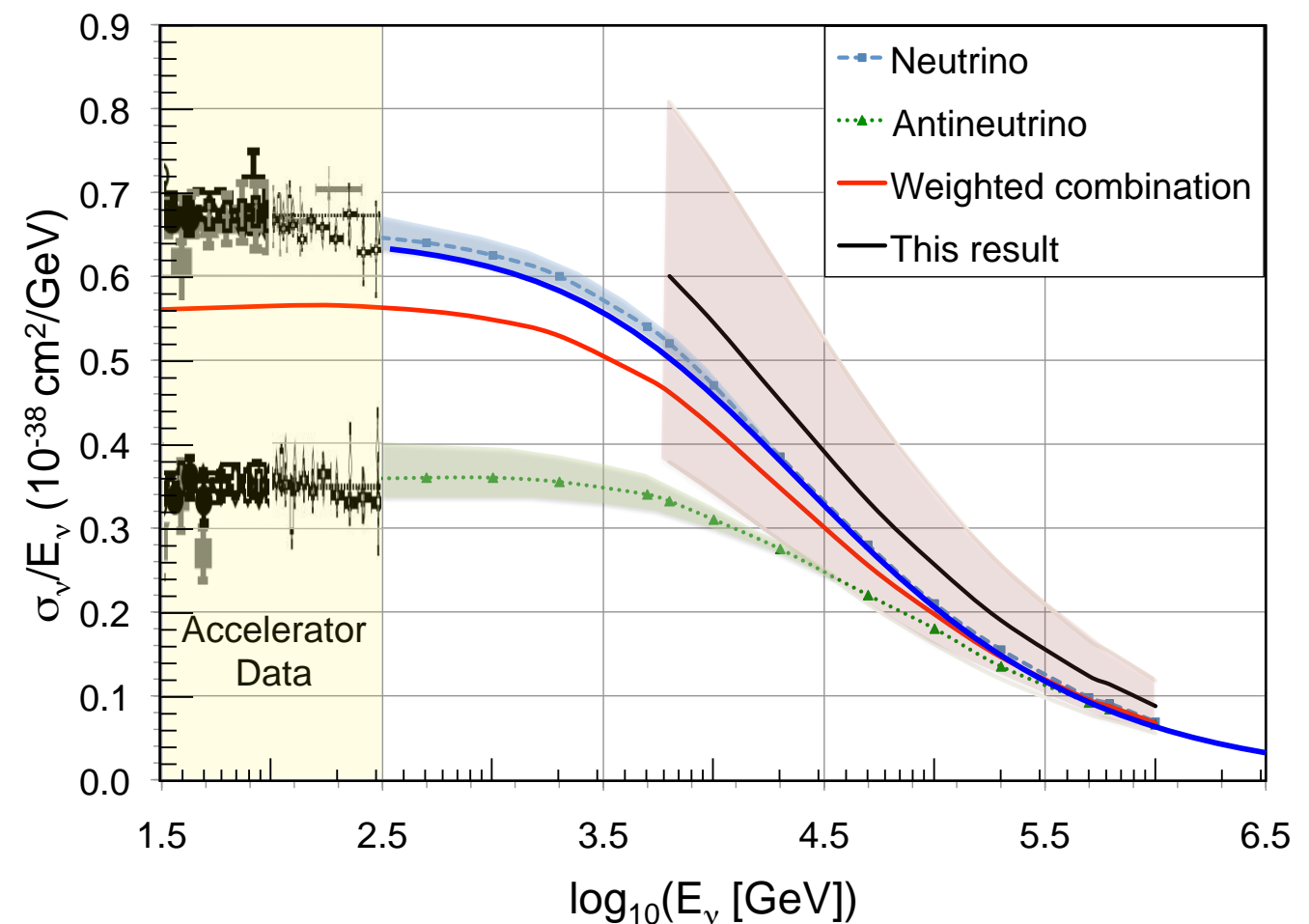
Neutrino cross sections

Kwiecinski, Martin, AS



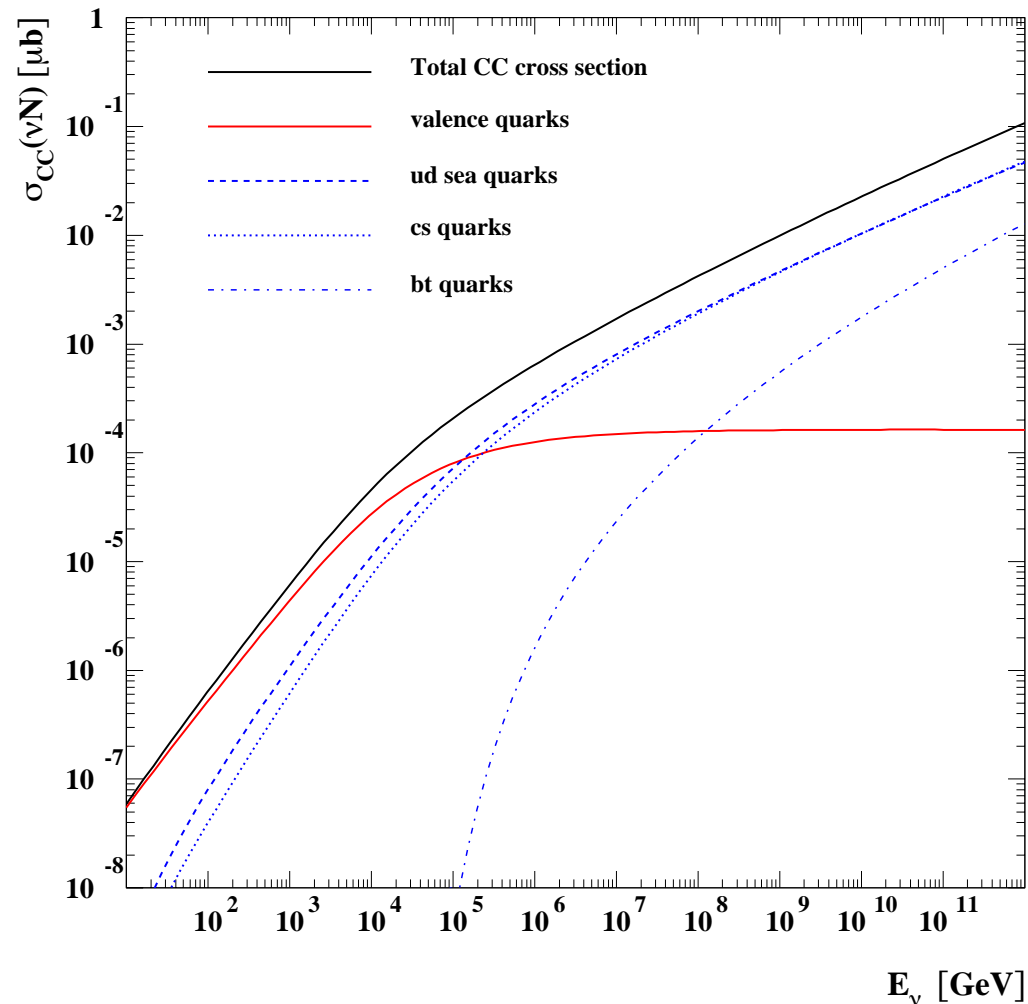
Calculation of the neutrino cross section using unified DGLAP/BFKL evolution: including small x resummation effects.

ICECUBE result



Neutrino cross sections

Kwiecinski, Martin, AS



Resummation predictions are very stable:
consistent with the more recent standard
DGLAP extrapolations and the new
measurement by the ICECUBE collaboration
(the sampled x values are not very small for
this kinematics though)

Calculation of the neutrino cross section
using unified DGLAP/BFKL evolution:
including small x resummation effects.

